*Current Research (2009) Newfoundland and Labrador Department of Natural Resources*
*Geological Survey, Report 09-1, pages 271-288*

# GEOCHEMICAL CHARACTERISTICS OF THE ORDOVICIAN VOLCANO-SEDIMENTARY ROCKS IN THE MARY MARCH BROOK AREA

A. Zagorevski and N. Rogers
Geological Survey of Canada, 601 Booth Street, Ottawa, ON, K1A 0E8

## ABSTRACT

*The Mary March Brook area, which forms part of the Buchans–Roberts Arm belt, is considered to be very prospective for volcanogenic massive sulphide (VMS) deposits. Detailed outcrop investigations and interpretation of geomagnetic data allowed a revision of the tectonostratigraphic relationships, including the subdivision of the volcanic rocks into the Harry's River ophiolite complex, Mary March Brook and Seal Pond formations of the Buchans–Roberts Arm belt, and the Red Indian Lake group. New lithogeochemical data presented herein support the revision and subdivision, and highlights the differences in the chemical characteristics and tectonic setting of these tectonostratigraphic units. The Harry's River ophiolite complex is dominated by back-arc basin basalts, and the Mary March Brook and Seal Pond formations by tholeiitic bimodal volcanic rocks interpreted to represent a rifted-arc environment; whereas the Red Indian Lake group is a bimodal calc-alkaline arc-volcanic sequence. The boundaries between the tectonostratigraphic units are folded thrust faults. The identification of distinct geochemical fingerprints in these tectonostratigraphic units has important implications for the distribution of mineral-deposit-bearing terranes in the Buchans–Roberts Arm belt.*

## INTRODUCTION

The Ordovician Buchans–Roberts Arm belt forms part of a tectonic collage of arc and back-arc terranes that were accreted to the Laurentian margin during the Middle and Late Ordovician (Figure 1; *e.g.*, Lissenberg *et al.*, 2005) and subsequently deformed during the Salinic Orogeny (*e.g.*, Dunning *et al.*, 1990). Detailed studies of the Buchans–Roberts Arm belt have delineated multiple fault-bound volcanic tracts that possess individual stratigraphic and tectonic histories, warranting their interpretation as separate terranes (*e.g.*, Bostock, 1988; Pope *et al.*, 1991; Kerr, 1996; Swinden *et al.*, 1997; O'Brien, 2003, 2007; Zagorevski *et al.*, 2006). Regional correlation of these terranes is often tenuous, as they are commonly incompletely characterized and many of their features resemble those of the adjacent terranes.

In this contribution, the geochemical characteristics of a sample suite for the Mary March area are examined, which, in comparison to most of the Buchans–Roberts Arm belt, has a well-exposed section of bedrock, and the previously proposed tectonostratigraphic subdivision is tested (Zagorevski and Rogers, 2008). The results of this study show that the tectonostratigraphic units in the Mary March Brook area have distinct geochemical fingerprints that can be utilized for regional terrane correlation. These geochemical fingerprints stem from distinct tectonic settings at the time of eruption of the volcanic rocks. Unravelling the tectonostratigraphy and structural history has significant implications for mineral exploration because the study area is host to a number of base-metal prospects.

## STRATIGRAPHY

Zagorevski and Rogers (2008) proposed several informal units in the areas covered by the Buchans (12A/15) and Badger (12A/16) NTS map areas. These include the Mary March Brook and the Seal Pond formations, which form part of the Buchans Group, but may have affinities with the Robert's Arm Group terranes. In addition, some units previously included in the Buchans Group (Kean, 1979; Kean and Jayasinghe, 1980; Thurlow and Swanson, 1981) have been provisionally re-assigned to the Red Indian Lake group (Rogers *et al.*, 2005a, b; Zagorevski *et al.*, 2006) and to the informally proposed Harry's River ophiolite complex (Zagorevski and Rogers, 2008).

### HARRY'S RIVER OPHIOLITE COMPLEX

The Harry's River ophiolite complex structurally underlies the Hungry Mountain Complex along the Hungry Mountain thrust (Figure 2). It is characterized by highly deformed pillow basalt, gabbro and diabase that were affected by predominantly amphibolite-facies metamorphism.

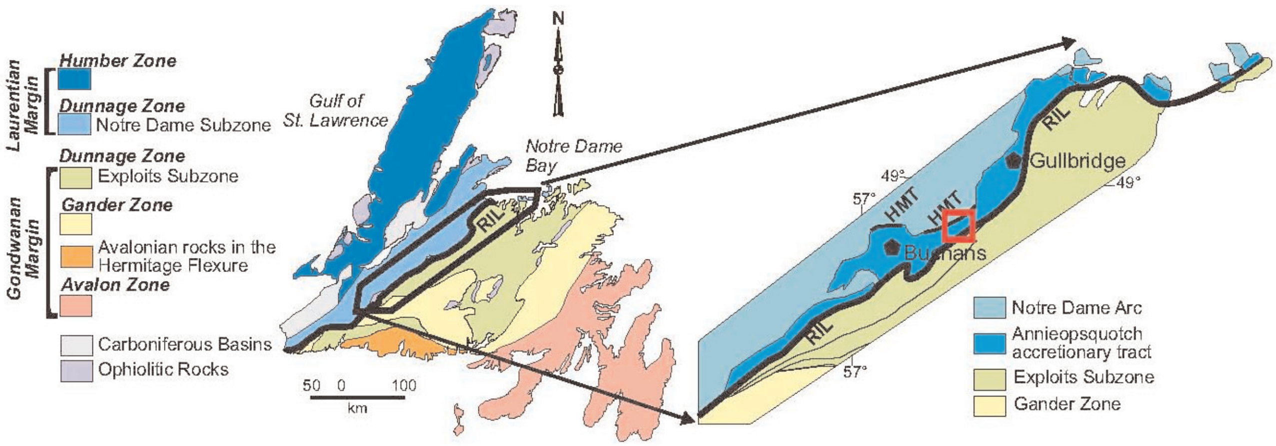


**Figure 1.** *Tectonostratigraphic zones of the Newfoundland Appalachians (modified after Williams* et al.*, 1988) and subdivision of the Notre Dame Subzone into the Notre Dame Arc and Annieopsquotch accretionary tract (modified from van Staal* et al.*, 1998). HMT–Hungry Mountain thrust, RIL–Red Indian Line. Location of the study area is indicated by the red polygon.*

## MARY MARCH BROOK FORMATION

The Mary March Brook and Seal Pond formations structurally underlie the Harry's River ophiolite complex and are characterized by pervasively altered bimodal volcanic rocks. Felsic volcanic rocks of the Mary March Brook formation form flow-and-dome complexes and display a wide range of volcanic textures and colours; however strongly porphyritic felsic volcanic rocks are rare. Mafic volcanic rocks are locally hematitic pillow lavas and breccias with common interpillow white to hematitic chert. These rocks are commonly strongly altered, chloritized and/or converted to epidosite. Rare mafic-derived sandstones are locally exposed, notably on Mary March Brook. Mafic and felsic rocks of the Mary March Brook formation are interfingered on a regional scale.

## SEAL POND FORMATION

The Seal Pond formation is characterized by quartz glomeroporphyritic to megacrystic rhyolite at its stratigraphic (or structural?) base. The remainder of the Seal Pond formation generally comprises quartz ± feldspar porphyritic felsic volcanic rocks including grey to reddish-brown flow-banded rhyolite and orange tuff to tuff breccia and minor pillow basalt. The Seal Pond formation in this area is characterized by much better defined lenticles of mafic volcanic rocks than that seen in the Mary March Brook formation. The rhyolite and shallow intrusive rocks petrographically resemble the Sandy Lake and 'Feeder' granodiorite intrusions of the Buchans area (Thurlow and Swanson, 1987). The Seal Pond formation hosts several zones of strongly altered volcanics, including two strongly pyritized rhyolite breccia outcrops in which trace base-metal sulphides were observed and noted.

## RED INDIAN LAKE GROUP

The rocks situated in the southern part of the study area were initially assigned to the Buchans Group (Thurlow and Swanson, 1981) but were later reassigned to the Red Indian Lake group (Rogers *et al.*, 2005b; Zagorevski and Rogers, 2008). The *ca.* 466–462 Ma Red Indian Lake group comprises calc-alkaline felsic volcanic rocks of the Healy Bay formation and tholeiitic to calc-alkaline mafic volcanic rocks of the Harbour Round formation (Rogers *et al.*, 2005b; Zagorevski *et al.*, 2006). The whole-rock chemical characteristics of the calc-alkaline portion of the Red Indian Lake group are similar to those of the Buchans Group, however some geochemical and isotopic differences have been discerned (Zagorevski and Rogers, 2008).

The Red Indian Lake group comprises a lower mafic sequence and an upper felsic sequence. The lower mafic sequence is dominated by pillow basalts locally associated with dacite and siliciclastic sandstone. The upper felsic sequence is dominated by felsic pyroclastic and epiclastic rocks and comprises laminated, bedded to massive ash to lapilli tuff and epiclastic rocks locally interbedded with multicoloured chert and minor rhyolite. The common presence of emerald to light-green chert fragments, chert beds and replacement horizons distinguishes this unit from the tuffaceous felsic rocks in the Buchans Group, Mary March Brook and Seal Pond formations (Zagorevski and Rogers, 2008).

## POST-ORDOVICIAN DYKES

A post-Silurian mafic dyke swarm has been documented throughout the area on the basis of outcrop observations and interpretation of geophysical data (Zagorevski and

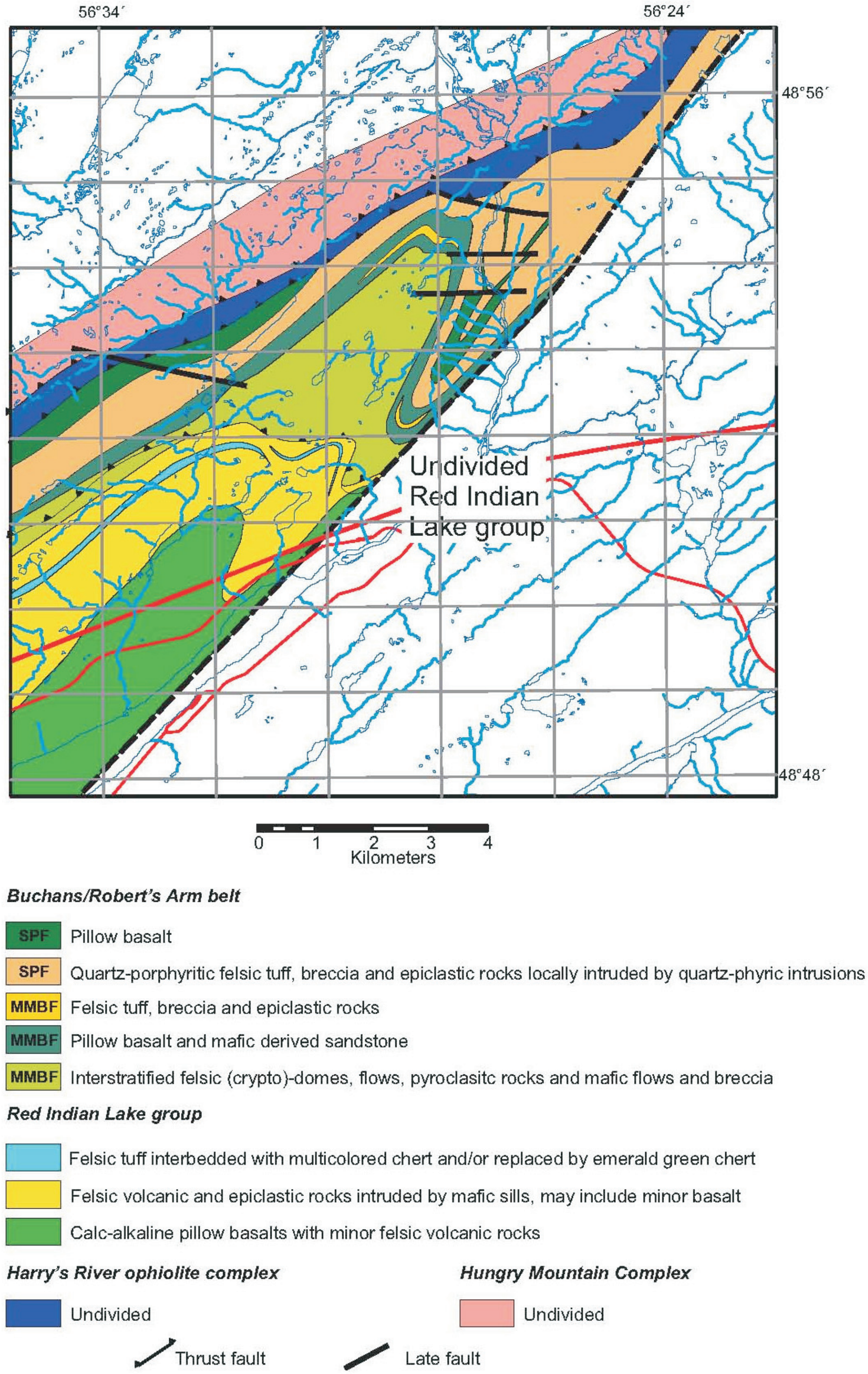


**Figure 2.** *Geology of the Mary March Brook area (modified after Zagorevski and Rogers, 2008). SPF–Seal Pond formation; MMBF–Mary March Brook formation.*

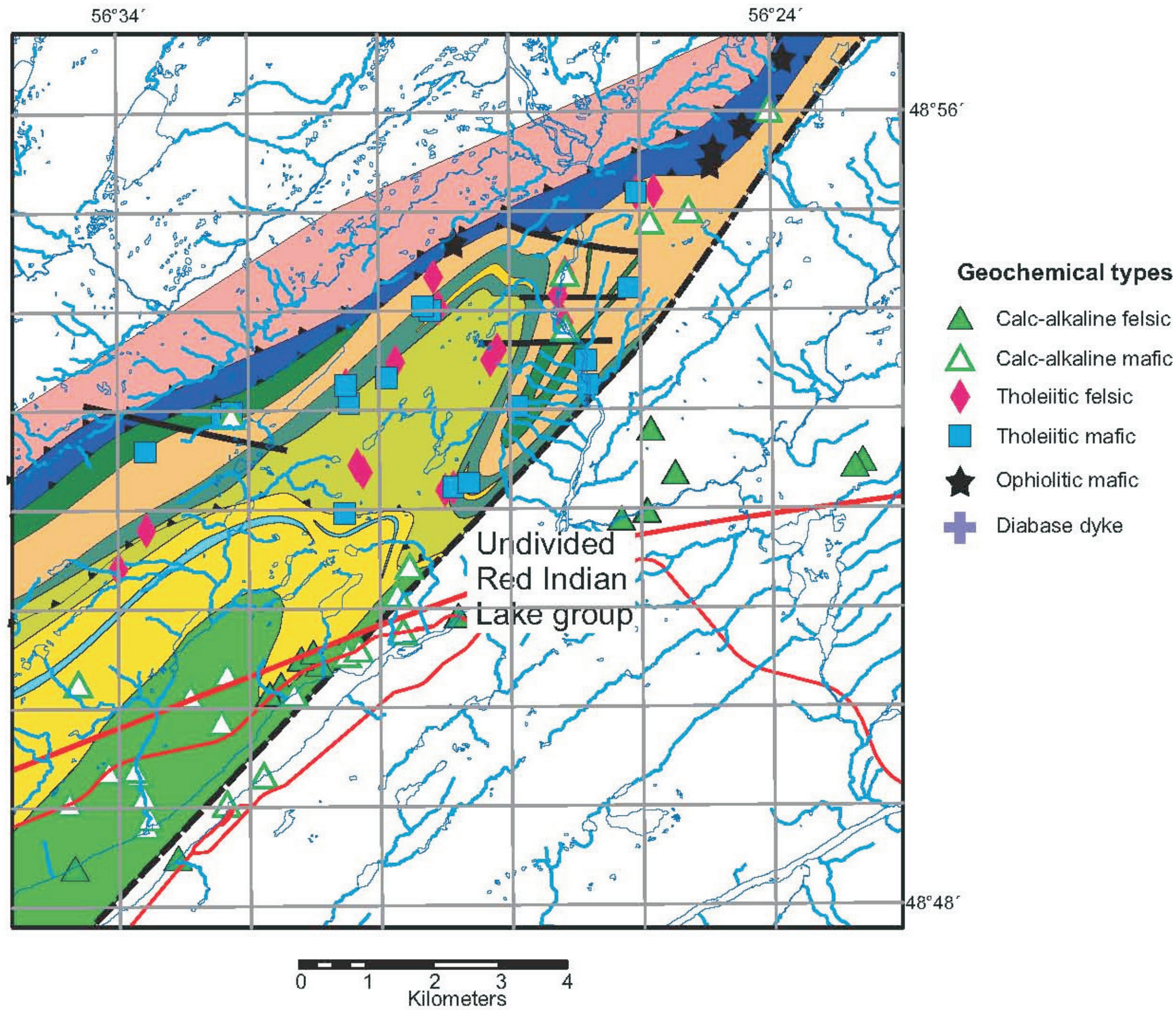


**Figure 3.** *Areal distribution of the geochemical types defined in this study.*

Rogers, 2008). These dykes are compositionally and texturally distinct from the probable feeder dykes of the host sequences, in that they are unaltered and undeformed. The dykes commonly contain megacrystic plagioclase and gabbroic pegmatite xenoliths or cognate enclaves.

## GEOCHEMISTRY

The geochemical characteristics of the study area are investigated on the basis of sixty-eight new analyses (Zagorevski, 2008) and fourteen compiled analyses (Davenport *et al.*, 1996; Rogers, 2004). The reader is referred to these sources for details of analytical methods. The distribution of samples is shown in Figure 3. The study area is underlain by a variety of geochemical rock types that are described in this section on the basis of major- and trace-element geochemistry (Appendix 1) as well as tectonic setting. The samples display a clear bimodal distribution comprising mainly basaltic and rhyodacitic compositions (Figure 4). The felsic and mafic volcanic rocks are subdivided into tholeiitic and calc-alkaline groups. In addition, two other mafic divisions have been made that have been separated on the basis of their outcrop association with ophiolitic rocks and crosscutting relationships.

### CALC-ALKALINE FELSIC ROCKS

Calc-alkaline felsic rocks comprise felsic flows, breccia, tuff and felsic dykes that plot in the rhyodacite to rhyolite fields of standard geochemical rock discrimination plots (Figure 4), and mainly occur in the southeastern part the study area (Figure 3). This geochemical group is characterized by strong enrichment of LREE on N-MORB and chondrite-normalized trace-element spidergrams (Figures 5 and 6). In addition, there are strong Th enrichment, prominent negative Nb and Ti anomalies and slight to prominent enrichment of Zr and Hf on N-MORB-normalized trace-element spidergrams (Figure 5), as well as marked enrichment

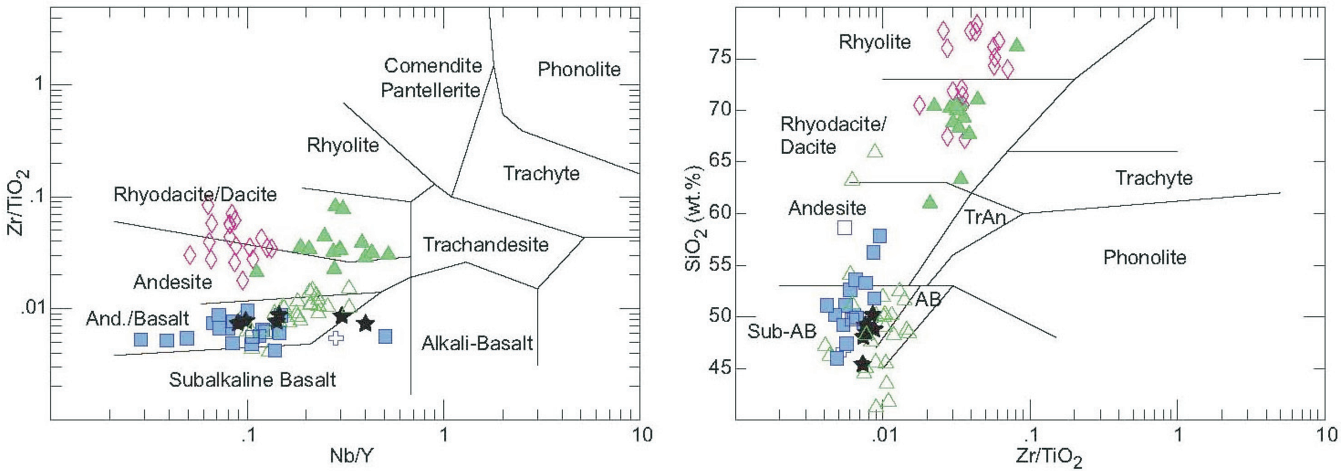


**Figure 4.** *Geochemical characteristics of the Mary March Brook area (discrimination plots after Winchester and Floyd, 1977). Symbols correspond to the geochemical types described in text.*

of Nb relative to HREE (Figure 6). The samples plot in the volcanic arc and syn-collisional field on tectonic discrimination plots (Figure 7).

## CALC-ALKALINE MAFIC ROCKS

Calc-alkaline mafic rocks comprise pillow and massive flows, pillow breccia and mafic dykes that have compositions ranging from basalt to basaltic andesite (Figure 4); they mostly occur in the southeastern part of the study area (Figure 3). Similar to the associated felsic rocks, this geochemical group is characterized by strong Th and LREE enrichment, strong Nb depletion, slight Ti depletion and notable enrichment of Nb relative HREE on N-MORB-normalized trace-element spidergrams (Figures 6 and 7). This group plots predominantly in the calc-alkaline basalt and plate margin basalt fields on tectonic discrimination plots (Figure 7).

## THOLEIITIC FELSIC ROCKS

Tholeiitic felsic rocks comprise felsic flows, breccia, tuff and felsic dykes of rhyodacite to rhyolite composition (Figure 4) and they occur only in the northwest (Figure 3). This geochemical group is characterized by a slightly LREE-enriched and Eu-depleted profile on chondrite-normalized, trace-element spidergrams (Figure 5). In addition, there is enrichment of Th, depletion of Nb and Ti and slight to prominent enrichment of Zr and Hf on N-MORB-normalized trace-element spidergrams (Figure 5). There is no significant enrichment of Nb relative to HREE (Figure 6). The samples plot in the volcanic-arc field and ocean-ridge granite fields on tectonic discrimination plots (Figure 7).

## THOLEIITIC MAFIC ROCKS

Tholeiitic mafic rocks comprise pillowed and massive flows, pillow breccia and mafic dykes of basalt to basaltic andesite composition (Figure 4) that occur exclusively in the northwest (Figure 3). This geochemical group is characterized by flat to LREE-enriched profile, Th enrichment, moderate Nb depletion, slight Ti depletion on N-MORB-normalized trace-element spidergrams (Figures 6 and 7). This group plots predominantly in the volcanic-arc tholeiite and back-arc basin basalt fields on tectonic discrimination plots (Figure 7).

## OPHIOLITIC MAFIC ROCKS

Ophiolitic rocks comprise pillow basalt, diabase and gabbro of basaltic composition (Figure 4) that occur exclusively in the northwest (Figure 3). This geochemical type is characterized by strong Th and LREE enrichment and a very small negative Nb anomaly on N-MORB-normalized trace-element spidergrams (Figure 8); Nb is enriched relative to HREE (Figures 6 and 8). This group plots in the fields of island-arc tholeitte, back-arc, continental-rift and within-plate settings on tectonic discrimination diagrams (Figure7).

## LATE DIABASE ROCKS

A single sample obtained from part of the late diabase dyke swarm has LREE enrichment and no Nb anomaly on N-MORB-normalized trace-element spidergrams (Figures 4, 6 and 8). This sample plots in the within-plate field on tectonic discrimination plots (Figure 7).

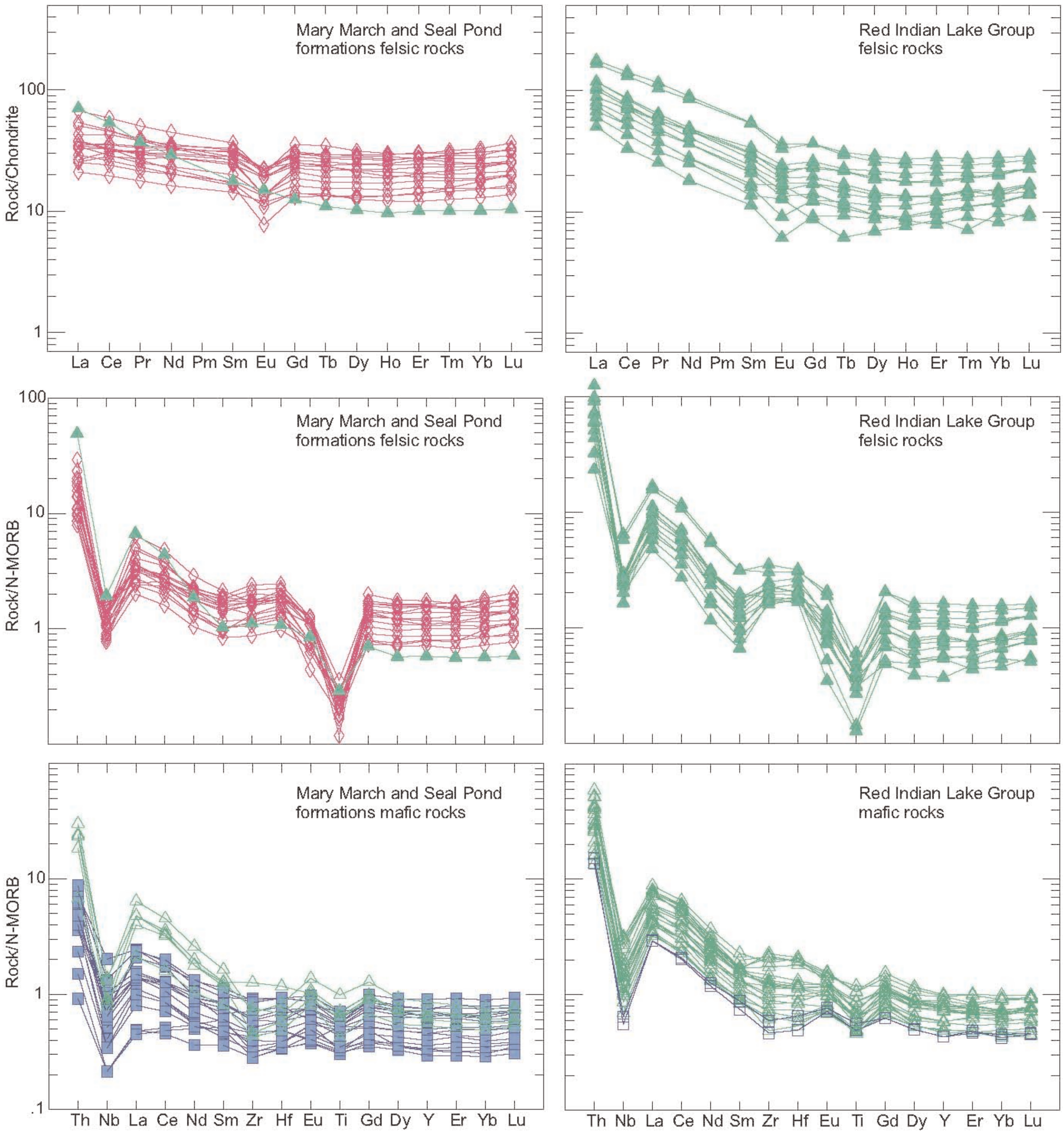


**Figure 5.** *Extended rare-earth-element (REE) spidergrams of the non-ophiolitic chemical groups defined in this study (normalization factors after Sun and McDonough, 1989).* See *Figure 4 for symbol legend.*

## DISCUSSION

The Mary March area was subdivided into lithologically distinct units belonging to the Harry's River ophiolite complex, Mary March Brook, Seal Pond formations, and Red Indian Lake group (Zagorevski and Rogers, 2008). These divisions are now also defined using the geochemical characteristics outlined above. In this section, the distribution of the geochemical characteristics within the lithologically distinct units, described in the previous section, is discussed and some of the tectonic implications are examined.

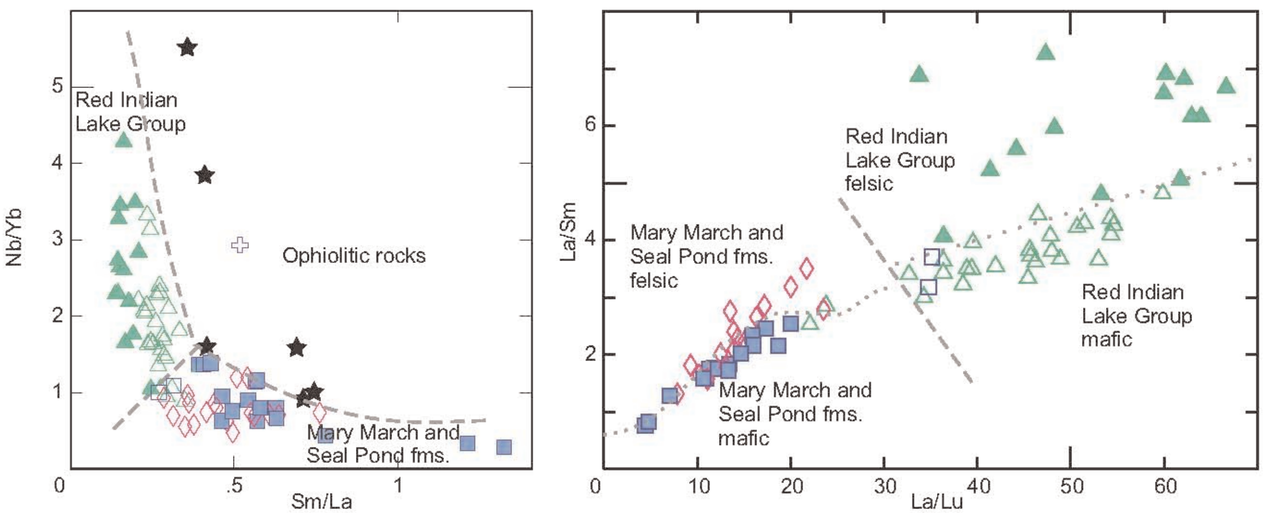


**Figure 6.** *Geochemical groups in the Mary March Brook area display different and distinct degrees of enrichment of LREE and Nb relative to MREE and HREE.*

## HARRY'S RIVER OPHIOLITE COMPLEX

The Harry's River ophiolite complex is a very distinctive unit, mainly due to its predominantly amphibolite-facies metamorphism and high magnetic susceptibility owing to the presence of magnetite. The eastern boundary of the Harry's River ophiolite complex with the adjacent Mary March Brook and Seal Pond formations is marked by a high-strain zone. Hence, no stratigraphic relationships can be inferred between these units. In addition, the geochemical characteristics of the ophiolite are distinct from all other units in the study area. The samples closely resemble E-MORB, however they do appear to have some traits consistent with a supra-subduction zone signature (Figures 7 and 8). These rocks compare closely to modern volcanic rocks erupted in a back-arc setting, such as the East Scotia Ridge (Leat *et al.*, 2000; Fretzdorff *et al.*, 2002). Hence, this portion of the Harry's River ophiolite complex is interpreted to represent a tectonic sliver of a peri-Laurentian back-arc basin. Similar slivers have been identified to the southwest of the study area, where the Otter Brook Suite of the Lloyds River ophiolite complex forms an excellent geochemical correlative and occupies a similar structural position (Zagorevski *et al.*, 2006).

## MARY MARCH BROOK AND SEAL POND FORMATIONS

The bimodal volcanic rocks of the Mary March Brook and the stratigraphically overlying Seal Pond formations structurally underlie the Harry's River ophiolite complex. The formations were separated on the basis of, 1) petrographic characteristics of the mafic volcanic rocks, 2) petrographic characteristics of the erupted felsic volcanic rocks, 3) preliminary geochemical results that suggested subtle geochemical differences, and 4) differences in magnetic susceptibility of the volcanic rocks (Zagorevski, 2008).

The igneous rocks of the Mary March Brook and Seal Pond formations have predominantly tholeiitic characteristics (Figure 7). Primitive island-arc tholeiite basalts occur near the interpreted stratigraphic base of the section. The amount of LREE- and Th-enrichment tends to become more prominent in the stratigraphically higher basalts, but there is no systematic increase in these parameters. The stratigraphically highest basalt lenticle of the Seal Pond formation has a calc-alkaline affinity. A similar relationship has been observed in felsic volcanic rocks. Tholeiitic felsic volcanic rocks occur at the base of the section, whereas the calc-alkaline rocks occur near the stratigraphic top of the Seal Pond formation. Gabbro and diabase that intrude the Seal Pond formation have calc-alkaline characteristics. The rhyolite and shallow-level intrusive rocks in the Seal Pond formation have previously been noted to be petrographically similar to the Sandy Lake and 'Feeder' granodiorite intrusions (Zagorevski and Rogers, 2008). However, comparison of the geochemical characteristics of the Sandy Lake intrusion (Zagorevski, 2008) with the tholeiitic felsic rocks in Seal Pond formation reveals significant differences (Figure 8), suggesting that these units are not related.

The eruption of island-arc tholeiite basalt and rhyolite suggests a highly rifted-arc setting. The geochemical characteristics broadly support the subdivision of the Mary March area into the Mary March Brook and Seal Pond formations, although there is no obvious geochemical change at the inferred boundary.

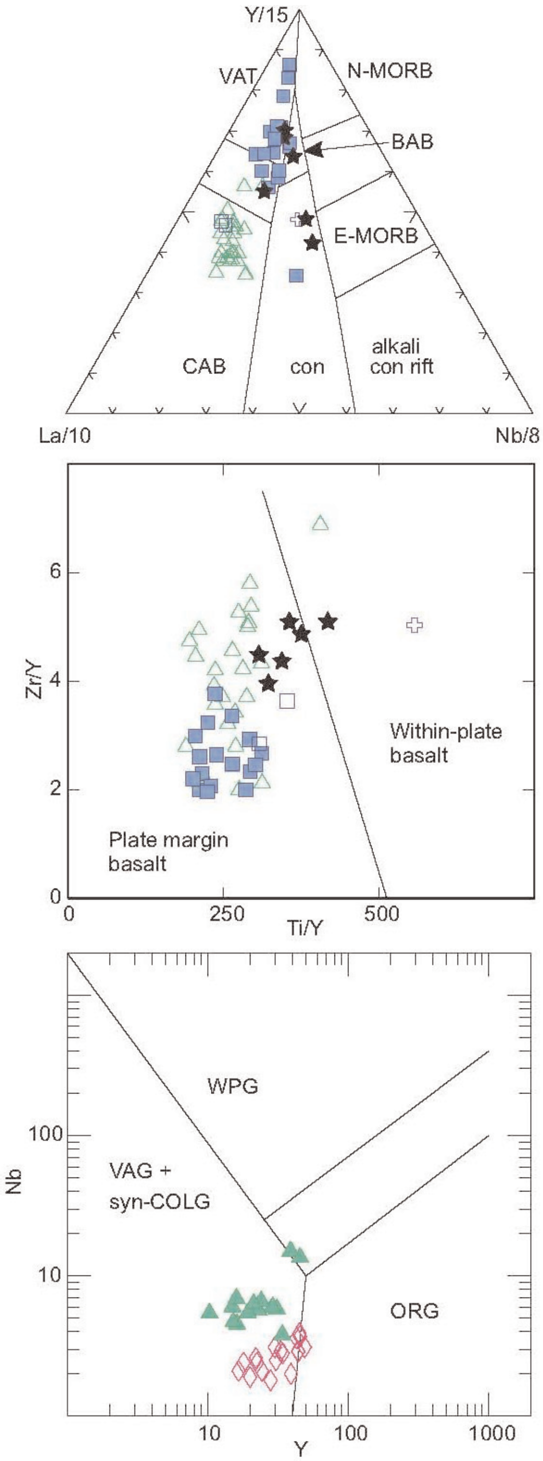


**Figure 7.** (adjacent) *The La/10–Y/15–Nb/8 and Ti/Y vs. Zr/Y tectonic setting discrimination plots for mafic volcanic rocks (Pearce and Gale, 1977; Cabanis and Lecolle, 1989); Nb-Y discrimination diagram for felsic rocks of the Healy Bay formation (Pearce* et al.*, 1984). BAB–back-arc basalt, CAB–calc-alkaline basalt, E-MORB–enriched mid-ocean-ridge basalt, N-MORB–normal mid-ocean-ridge basalt, ORG–ocean-ridge granite, syn-COLG–syn-collisional granite, VAG–volcanic arc granite, VAT–volcanic arc tholeiite, WPG–within-plate granite.* See *Figure 6 for symbol legend.*

## RED INDIAN LAKE GROUP

The Red Indian Lake group is separated from the Mary March Brook formation by a thin brittle-ductile shear zone that marks a thrust boundary (Zagorevski and Rogers, 2008). It is characterized by a lower bimodal unit that contains uniform calc-alkaline mafic and felsic volcanic rocks. The upper unit comprises predominantly felsic pyroclastic and epiclastic tuffaceous rocks locally interbedded with chert and jasperite that locally contain radiolaria. The epiclastic volcanic rocks have not been sampled in the study area due to likelihood of sedimentary contamination of the volcanic geochemical signatures. Associated rhyolite exposed to the southwest of the study area, however, has a calc-alkaline affinity (Zagorevski, 2008). A single sample taken from a diabase sill that intrudes the felsic tuffaceous sequence also displays calc-alkaline chemical characteristics, although the age of the diabase relative to these rocks is unknown.

The geochemical characteristics of the Red Indian Lake group are consistent with a volcanic sequence formed above continental crust as indicated by highly negative εNd values and abundant zircon inheritance in the felsic volcanic rocks (Zagorevski *et al.*, 2006; A. Zagorevski and N. Rogers, unpublished data, 2009). Following the nomenclature of Rogers *et al.* (2005b) and Zagorevski *et al.* (2006), these rocks are subdivided between the upper calc-alkaline basalt member of the Harbour Round formation and the felsic tuff dominated Healy Bay formation.

### POST-ORDOVICIAN DYKES

The analyzed, within-plate, diabase dyke forms a part of an east–west dyke swarm that is irregularly distributed throughout central Newfoundland. These dykes cut across folds and are locally coincident with east–west dip-slip faults (Zagorevski and Rogers, 2008). The distribution of the dyke swarm, as indicated on regional aeromagnetic maps (*i.e.*, Dumount and Potvin, 2007a, b), suggests that they formed in response to a regional-scale north–south extensional event, which postdates the Ordovician Taconic and Ordovician–Silurian Salinic deformation in the Buchans–Roberts Arm belt.

## CONCLUSIONS

Detailed study of the Mary March area has delineated three fault-bounded volcanic tracts each of which has a dis-

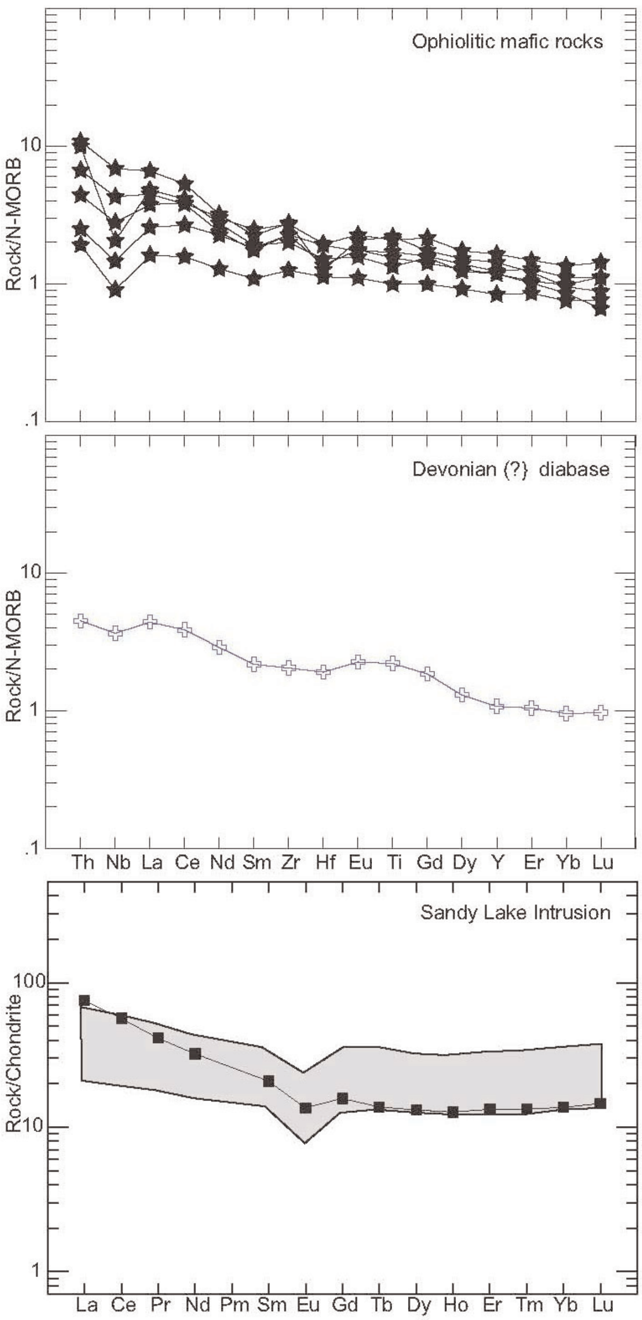


**Figure 8.** *Extended rare-earth-element (REE) spidergrams of the ophiolitic metabasites, late diabase dyke and comparison of felsic volcanic rocks in the Mary March Brook and Seal Pond formations, and the Sandy Lake intrusion indicated by solid squares (normalization factors after Sun and McDonough, 1989).*

tinct internal stratigraphy and tectonic history, warranting their interpretation as separate terranes. The geochemical data presented in this report support the distinctions based on field mapping, *i.e.*, the Mary March Brook and Seal Pond formations are dominated by tholeiitic rocks, and the Red Indian Lake group is dominated by calc-alkaline rocks. The Harry's River ophiolite complex is inferred to have formed in a back-arc basin, the Mary March Brook and Seal Pond formations are inferred to have formed in a rifted-arc setting, whereas the Red Indian Lake group represents a calc-alkaline arc. The VMS mineralization of the Connel option, Mary March zone (Mary March Wilderness Park area), and Buchans Junction North prospects occurs in the calc-alkaline volcanic rocks of the Red Indian Lake group, whereas the Seal Pond and Beaver Pond prospects occur in the Mary March Brook formation (Zagorevski and Rogers, 2008). The association of these mineral prospects within different terranes indicates that the structural repetition of mineralization cannot be universally attributed to the imbrication of a single stratigraphic horizon. Rather, mineralization has occurred in each of the terranes on at least one occasion, and these have subsequently been tectonically juxtaposed. The consequence of this is that no one exploration model can be applied throughout the Buchans–Roberts Arm belt, as petrographically similar sequences occur within each of the terranes.

The identification of the geochemical fingerprints of these terranes in the area of relatively good exposure improves understanding of the volcanic associations in the areas of poor exposure and/or structural complexity. Improved correlations to other regional tracts such as the Lloyds River ophiolite complex and Red Indian Lake group (Zagorevski *et al.*, 2006) enables establishment of a testable regional tectonostratigraphic framework that can be used as a guide to exploration. Subsequent work will focus on extending these subdivisions into the less well-exposed portions of the Buchans–Roberts Arm belt.

## ACKNOWLEDGMENTS

The authors would like to acknowledge the contribution of the Geological Survey of Newfoundland and Labrador for their assistance and support in conducting this research. In particular we would like to thank A. Kerr and B. O'Brien for fieldtrips and discussions of the peculiarities of the Buchans–Roberts Arm belt. The scope of this manuscript has been improved through reviews by C.R. van Staal and A. Kerr. This work was supported by and is a contribution to the Geological Survey of Canada Targeted Geoscience Initiative 3 Program (GSC Contribution # 20080587).

## REFERENCES

Bostock, H.H.
1988: Geology and petrochemistry of the Ordovician volcano-plutonic Robert's Arm Group, Notre Dame Bay, Newfoundland. Geological Survey of Canada Bulletin 369, Geological Survey of Canada, 84 pages.

Cabanis, B. and Lecolle, M.
1989: Le diagramme La/10-Y/15-Nb/8; un outil pour la discrimination des series volcaniques et la mise en evidence des processus de melange et/ou de contamination crustale. The La/10-Y/15-Nb/8 diagram; a tool for distinguishing volcanic series and discovering crustal mixing and/or contamination. Comptes Rendus de l'Academie des Sciences, Serie 2, Mecanique, Physique, Chimie, Sciences de l'Univers, Sciences de la Terre, Volume 309, No. 20, pages 2023-2029.

Davenport, P.H., Honarvar, P., Hogan, A., Kilfoil, G., King, D., Nolan, L.W., Ash, J.S., Colman-Sadd, S.P., Hayes, J.P., Liverman, D.G.E., Kerr, A. and Evans, D.T.W.
1996: Digital geoscience atlas of the Buchans-Robert's Arm belt, Newfoundland. Newfoundland Geological Survey Branch.

Dumount, R. and Potvin, J.
2007a: First vertical derivative of the magnetic field, Gullbridge Aeromagnetic Survey; Newfoundland and Labrador, parts of NTS 12 A/15 and A/16. Geological Survey of Canada, Open File 5652, scale 1:25,000.

2007b: Residual total magnetic field, Gullbridge Aeromagnetic Survey; Newfoundland and Labrador, parts of NTS 12 A/15 and A/16. Geological Survey of Canada, Open File 5647, scale 1:25,000.

Dunning, G.R., O'Brien, S.J., Colman-Sadd, S.P., Blackwood, R.F., Dickson, W.L., O'Neill, P.P. and Krogh, T.E.
1990: Silurian orogeny in the Newfoundland Appalachians. Journal of Geology, Volume 98, No. 6, pages 895-913.

Fretzdorff, S., Livermore, R.A., Devey, C.W., Leat, P.T. and Stoffers, P.
2002: Petrogenesis of the back-arc East Scotia Ridge, South Atlantic Ocean. Journal of Petrology, Volume 43, No. 8, pages 1435-1467.

Kean, B.F.
1979: Buchans (12A/15), Newfoundland, scale 1:50,000.

Kean, B.F. and Jayasinghe, N.R.
1980: Badger map area (12A/16), Newfoundland. Government of Newfoundland and Labrador, Department of Mines and Energy, Mineral Development Division, Report 80-1, pages 37-43.

Kerr, A.
1996: New perspectives on the stratigraphy, volcanology, and structure of island-arc volcanic rocks in the Ordovician Roberts Arm Group, Notre Dame Bay. *In* Current Research. Newfoundland Department of Mines and Energy, Report 96-1, pages 283-310.

Leat, P.T., Livermore, R.A., Millar, I.L. and Pearce, J.A.
2000: Magma supply in back-arc spreading centre segment E2, East Scotia Ridge. Journal of Petrology, Volume 41, pages 845-866.

Lissenberg, C.J., Zagorevski, A., McNicoll, V.J., van Staal, C.R. and Whalen, J.B.
2005: Assembly of the Annieopsquotch accretionary tract, Newfoundland Appalachians; age and geodynamic constraints from syn-kinematic intrusions. Journal of Geology, Volume 113, No. 5, pages 553-570.

O'Brien, B.H.
2003: Geology of the central Notre Dame Bay region (Parts of NTS areas 2E/3,6,11) northestern Newfoundland. Governement of Newfoundland and Labrador, Department of Mines and Energy, Geological Survey, Report 03-03, 147 pages.

2007: Geology of the Buchans-Roberts Arm volcanic belt, near Great Gull Lake. *In* Current Research. Newfoundland and Labrador Department of Natural Resources, Geological Survey Branch, Report 07-1, pages 85-102.

Pearce, J.A. and Gale, G.H.
1977: Identification of ore-deposition environment from trace-element geochemistry of associated igneous host rocks. Institute of Mining Metallurgy, London, United Kingdom (GBR).

Pearce, J.A., Harris, N.B.W. and Tindle, A.G.
1984: Trace element discrimination diagrams for the tectonic interpretation of granitic rocks. Journal of Petrology, Volume 25, No. 4, pages 956-983.

Pope, A.J., Calon, T.J. and Swinden, H.S.
1991: Stratigraphy, structural geology and mineralization in the Gullbridge area, central Newfoundland. Geological Survey of Canada, Open File 2156, pages 93-100.

Rogers, N.
2004: Red Indian Line geochemical database. Geological Survey of Canada, Open File 4605.

Rogers, N., van Staal, C.R. and McNicoll, V.
2005a: Geology, Badger, Newfoundland (NTS 12-A/16), scale 1:50,000.

Rogers, N., van Staal, C.R., Pollock, J. and Zagorevski, A.
2005b: Geology, Lake Ambrose and part of Buchans, Newfoundland (NTS 12-A/10 and part of 12-A/15), scale 1:50,000.

Sun, S.S. and McDonough, W.F.
1989: Chemical and isotopic systematics of oceanic basalts; implications for mantle composition and processes: Geological Society, Special Publications, Volume 42, pages 313-345.

Swinden, H.S., Jenner, G.A. and Szybinski, Z.A.
1997: Magmatic and tectonic evolution of the Cambrian-Ordovician Laurentian margin of Iapetus; geochemical and isotopic constraints from the Notre Dame Subzone, Newfoundland. Geological Society of America Memoir, Volume 191, pages 337-365.

Thurlow, J.G. and Swanson, E.A.
1981: Geology and ore deposits of the Buchans area, central Newfoundland. Geological Association of Canada, Special Paper 22, pages 113-142.

1987: Stratigraphy and structure of the Buchans Group. Geological Survey of Canada, Paper 86-24, pages 35-46.

van Staal, C.R., Dewey, J.F., Mac Niocaill, C. and McKerrow, W.S.
1998: The Cambrian-Silurian tectonic evolution of the Northern Appalachians and British Caledonides; history of a complex, west and southwest Pacific-type segment of Iapetus. *In* Lyell: The Past is the Key to the Present. *Edited by* D.J. Blundell and A.C. Scott. Special Publication, London, Geological Society, pages 199-242.

Williams, H., Colman-Sadd, S.P. and Swinden, H.S.
1988: Tectonic-stratigraphic subdivisions of central Newfoundland. Geological Survey of Canada, Paper 88-1B, pages 91-98.

Winchester, J.A. and Floyd, P.A.
1977: Geochemical discrimination of different magma series and their differentiation products using immobile elements. Chemical Geology, Volume 20, No. 4, pages 325-343.

Zagorevski, A.
2008: Preliminary geochemical database of the Buchans-Robert's Arm Belt, central Newfoundland: Geological Survey of Canada Open File 5986, 1 CD-ROM.

Zagorevski, A. and Rogers, N.
2008: Stratigraphy and structural geology of the Ordovician volcano-sedimentary rocks in the Mary March Brook area. *In* Current Research. Newfoundland and Labrador Department of Natural Resources, Geological Survey, Report 08-01, pages 111-123.

Zagorevski, A., Rogers, N., McNicoll, V., Lissenberg, C.J., van Staal, C.R. and Valverde-Vaquero, P.
2006: Lower to Middle Ordovician evolution of peri-Laurentian arc and back-arc complexes in the Iapetus: Constrains from the Annieopsquotch Accretionary Tract, central Newfoundland. Geological Society of America Bulletin, Volume 118, No. 3/4, pages 324-342.

# APPENDIX 1

## WHOLE-ROCK GEOCHEMISTRY OF THE MARY MARCH AREA, NAD 83, UTM ZONE 21

| **Sample** | **2141241** | **2141268** | **2343624** | **2343625** | **RAX01 060** | **RAX01 061** | **RAX01 062** | **RAX01 063** | **RAX01 064** | **RAX02 125** | **RAX02 127** | **RAX02 128** |
|---|---|---|---|---|---|---|---|---|---|---|---|---|
| Easting | 532106 | 536281 | 538051 | 538051 | 532918 | 533826 | 534506 | 535078 | 530989 | 545687 | 541653 | 535544 |
| Northing | 5407912 | 5410162 | 5417672 | 5417672 | 5406265 | 5407267 | 5407801 | 5409320 | 5406069 | 5413744 | 5412778 | 5409890 |
| geochem. Type* | CAB | CAB | EMORB | EMORB | CAB | CAB | CAB | CAB | CAB | CARD | CARD | CARD |
| strat. unit | RILG | RILG | HR | HR | RILG | RILG | RILG | RILG | RILG | RILG | RILG | RILG |
| $SiO_2$ | 45.50 | 41.20 | 50.20 | 45.40 | 58.61 | 41.80 | 49.97 | 48.26 | 49.73 | 76.17 | 68.83 | 68.28 |
| $TiO_2$ | 0.63 | 0.61 | 1.96 | 2.79 | 0.62 | 0.80 | 1.51 | 0.79 | 0.71 | 0.18 | 0.39 | 0.52 |
| $Al_2O_3$ | 12.00 | 13.32 | 13.90 | 14.00 | 11.56 | 14.30 | 16.24 | 16.54 | 13.80 | 13.08 | 14.12 | 14.75 |
| MnO | 0.12 | 0.36 | 0.32 | 0.39 | 0.50 | 0.13 | 0.14 | 0.16 | 0.18 | 0.06 | 0.13 | 0.07 |
| MgO | 1.89 | 6.20 | 4.85 | 5.79 | 7.95 | 5.87 | 5.97 | 5.94 | 5.28 | 0.71 | 1.71 | 0.99 |
| CaO | 21.56 | 13.35 | 9.07 | 10.60 | 4.70 | 12.55 | 5.24 | 8.48 | 10.28 | 1.03 | 3.07 | 1.45 |
| $Na_2O$ | 0.44 | 3.43 | 4.46 | 2.96 | 0.12 | 3.74 | 5.27 | 5.28 | 4.37 | 5.28 | 4.31 | 4.36 |
| $K_2O$ | 0.02 | 0.56 | 0.11 | 0.07 | 0.19 | 0.16 | 0.46 | 0.09 | 0.22 | 1.16 | 0.91 | 4.69 |
| $P_2O_5$ | 0.17 | 0.18 | 0.27 | 0.48 | 0.09 | 0.18 | 0.26 | 0.17 | 0.14 | 0.03 | 0.06 | 0.17 |
| LOI | 11.11 | 13.96 | 1.77 | 2.16 | 5.45 | 13.72 | 7.26 | 5.50 | 9.19 | 0.91 | 2.30 | 1.53 |
| $Fe_2O_3t$ | 6.72 | 8.25 | 11.90 | 14.70 | 10.06 | 7.86 | 8.93 | 10.06 | 7.04 | 1.55 | 3.97 | 3.33 |
| Total | 99.93 | 100.72 | 98.81 | 99.34 | 99.85 | 101.11 | 101.25 | 101.27 | 100.93 | 100.16 | 99.84 | 100.15 |
| Ba | 43 | 77 | 35 | 11 | 706 | 67 | 348 | 79 | 229 | 547 | 323 | 1322 |
| Cr | 387 | 466 | | | 35 | 323 | 81 | 38 | 208 | 27 | 3 | 35 |
| Cs | | | | | 0.96 | 0.77 | 0.96 | 0.06 | 0.11 | 0.65 | 0.70 | 0.42 |
| Cu | 17 | 77 | 110 | 155 | 3 | 63 | 76 | 107 | 74 | 7 | 8 | 12 |
| Ga | 18.0 | 14.0 | | | 10.9 | 12.0 | 17.3 | 13.8 | 9.9 | 11.7 | 14.6 | 15.1 |
| Hf | 1.7 | 1.5 | 2.8 | 2.6 | 1.0 | 2.3 | 4.0 | 1.8 | 1.3 | 3.9 | 3.6 | 4.1 |
| Nb | 3.0 | 3.0 | 10.0 | 16.0 | 1.3 | 3.4 | 7.4 | 3.1 | 1.5 | 5.4 | 5.4 | 6.3 |
| Ni | 152 | 186 | 17 | 8 | 40 | 156 | 8 | 36 | 92 | 3 | 3 | 5 |
| Pb | | | 3.0 | 4.0 | 6.7 | 1.0 | 2.7 | 5.0 | 1.0 | 43.8 | 5.9 | 7.1 |
| Rb | | | | 1.0 | 5.5 | 3.2 | 9.3 | 1.6 | 4.1 | 43.9 | 26.8 | 115.6 |
| Sc | 26 | 31 | 46 | 40 | 25 | 32 | 20 | 31 | 36 | 4 | 9 | 9 |
| Sr | 125 | 134 | 152 | 218 | 121 | 169 | 205 | 122 | 157 | 270 | 211 | 149 |
| Th | 3.20 | 3.30 | 0.80 | 1.30 | 1.82 | 3.60 | 4.42 | 3.52 | 1.64 | 8.46 | 2.80 | 11.77 |
| U | | | | | 0.49 | 1.19 | 1.40 | 1.02 | 0.54 | 2.19 | 1.20 | 2.96 |
| V | 173 | 192 | 326 | 423 | 231 | 223 | 179 | 463 | 257 | 12 | 56 | 83 |
| Y | 13 | 13 | 33 | 40 | 12 | 16 | 22 | 16 | 12 | 19 | 10 | 21 |
| Zn | 58 | 130 | 125 | 116 | 127 | 44 | 65 | 49 | 44 | 30 | 42 | 52 |
| Zr | 66 | 55 | 168 | 204 | 34 | 88 | 154 | 61 | 44 | 147 | 117 | 171 |
| La | 10.60 | 10.30 | 11.20 | 16.50 | 7.27 | 13.00 | 19.28 | 13.69 | 7.34 | 17.70 | 14.30 | 25.35 |
| Ce | 22.80 | 20.80 | 28.50 | 39.90 | 15.16 | 28.60 | 42.97 | 27.02 | 15.60 | 31.94 | 26.40 | 46.82 |
| Pr | 3.00 | 2.50 | 3.90 | 5.30 | 1.99 | 3.78 | 5.59 | 3.43 | 2.15 | 3.61 | 3.00 | 5.28 |
| Nd | 13.30 | 10.50 | 17.40 | 23.30 | 8.64 | 15.57 | 22.46 | 14.39 | 9.20 | 12.92 | 11.70 | 19.18 |
| Sm | 2.90 | 2.40 | 4.60 | 5.90 | 1.96 | 3.39 | 4.52 | 3.24 | 2.31 | 2.44 | 2.10 | 3.67 |
| Eu | 0.80 | 0.70 | 1.80 | 2.10 | 0.73 | 0.98 | 1.46 | 1.08 | 0.78 | 0.53 | 0.74 | 1.01 |
| Gd | 3.20 | 3.10 | 5.20 | 6.40 | 2.30 | 3.09 | 4.40 | 3.41 | 2.30 | 2.57 | 1.78 | 3.54 |
| Tb | 0.40 | 0.40 | 0.90 | 1.10 | 0.36 | 0.50 | 0.68 | 0.50 | 0.37 | 0.45 | 0.23 | 0.53 |
| Dy | 2.50 | 2.50 | 5.80 | 6.90 | 2.27 | 2.92 | 4.05 | 2.98 | 2.26 | 2.84 | 1.76 | 3.29 |
| Ho | 0.50 | 0.50 | 1.20 | 1.40 | 0.50 | 0.61 | 0.86 | 0.64 | 0.48 | 0.64 | 0.43 | 0.75 |
| Er | 1.40 | 1.40 | 3.00 | 3.60 | 1.44 | 1.91 | 2.40 | 1.86 | 1.38 | 2.02 | 1.42 | 2.28 |
| Tm | 0.20 | 0.20 | 0.40 | 0.50 | 0.21 | 0.27 | 0.37 | 0.27 | 0.21 | 0.34 | 0.18 | 0.38 |
| Yb | 1.30 | 1.40 | 2.60 | 2.90 | 1.29 | 1.78 | 2.22 | 1.89 | 1.38 | 2.37 | 1.65 | 2.32 |
| Lu | 0.20 | 0.20 | 0.30 | 0.40 | 0.21 | 0.29 | 0.35 | 0.27 | 0.21 | 0.37 | 0.23 | 0.42 |

*BAB-back-arc basalt; CAB -calc-alkaline basalt; CARD - Calc-alkaline rhyodacite; E-MORB-enriched mid-oceanic ridge basalt; IAT-island arc tholeiite, TRD-tholeiitic rhyodacite; WPB-within plate basalt

| RAX02 129 | RAX02 162 | RAX06 A001 | RAX06 A010A | RAX06 A011 | RAX06 A012 | RAX06 A013 | RAX06 A015 | RAX06 A016 | RAX06 A017 | RAX06 A020A | RAX06 A020B | RAX06 A029 | RAX06 A030 |
|---|---|---|---|---|---|---|---|---|---|---|---|---|---|
| 537110 | 545542 | 538729 | 537753 | 537604 | 537660 | 537466 | 536949 | 536788 | 536087 | 536036 | 536036 | 536243 | 536009 |
| 5410490 | 5413637 | 5415580 | 5416543 | 5416484 | 5417122 | 5416565 | 5415527 | 5415227 | 5414750 | 5415089 | 5415089 | 5413599 | 5412695 |
| CAB | CARD | TRD | TRD | IAT/BAB | TRD | IAT/BAB | TRD | IAT/BAB | IAT/BAB | IAT/BAB | TRD | TRD | IAT/BAB |
| RILG | RILG | MM | MM | MM | MM | MM | MM | MM | MM | MM | MM | MM | MM |
| 52.48 | 81.68 | 75.10 | 77.66 | 53.60 | 67.44 | 57.83 | 77.71 | 56.25 | 51.10 | 49.40 | 78.34 | 76.01 | 49.23 |
| 0.69 | 0.16 | 0.23 | 0.23 | 0.67 | 0.31 | 0.55 | 0.31 | 0.78 | 0.62 | 0.89 | 0.27 | 0.45 | 0.39 |
| 14.10 | 9.98 | 13.17 | 11.68 | 14.80 | 14.36 | 15.39 | 11.12 | 16.85 | 16.10 | 13.73 | 10.54 | 12.07 | 16.31 |
| 0.14 | 0.02 | 0.04 | 0.05 | 0.16 | 0.08 | 0.12 | 0.04 | 0.13 | 0.15 | 0.31 | 0.03 | 0.07 | 0.16 |
| 5.04 | 0.27 | 0.23 | 0.63 | 5.99 | 2.88 | 3.92 | 0.29 | 4.37 | 4.30 | 5.25 | 0.88 | 0.50 | 8.81 |
| 10.42 | 0.32 | 1.12 | 1.03 | 4.47 | 1.37 | 2.27 | 2.08 | 2.02 | 6.35 | 5.22 | 0.23 | 1.04 | 10.62 |
| 2.73 | 5.19 | 5.25 | 3.59 | 5.70 | 5.33 | 5.73 | 1.93 | 5.28 | 5.80 | 4.61 | 5.14 | 6.01 | 2.29 |
| 1.28 | 0.31 | 1.54 | 1.92 | 0.58 | 0.99 | 0.65 | 2.19 | 0.26 | 0.14 | 0.08 | 0.07 | 0.16 | 0.60 |
| 0.22 | 0.03 | 0.05 | 0.04 | 0.09 | 0.06 | 0.09 | 0.07 | 0.11 | 0.07 | 0.11 | 0.06 | 0.11 | 0.04 |
| 5.12 | 0.51 | 1.55 | 1.77 | 3.70 | 2.24 | 3.47 | 2.77 | 3.05 | 4.30 | 9.44 | 1.21 | 0.65 | 2.70 |
| 7.68 | 1.50 | 1.96 | 1.57 | 9.50 | 4.73 | 9.85 | 1.66 | 11.27 | 10.20 | 11.09 | 3.42 | 2.79 | 9.30 |
| 99.98 | 99.97 | 100.24 | 100.17 | 99.40 | 99.80 | 99.90 | 100.17 | 100.40 | 99.20 | 100.16 | 100.19 | 99.87 | 100.53 |
| 726 | 119 | 123 | 93 | 111 | 156 | 90 | 88 | 65 | 37 | 14 | 13 | 35 | 79 |
| 420 | 23 | | 19 | | 21 | | 15 | 9 | | | | | 311 |
| 0.41 | 0.24 | 0.57 | 0.65 | 0.14 | 0.16 | 0.19 | 0.27 | 0.06 | 0.05 | 0.07 | 0.03 | 0.06 | 0.29 |
| 69 | 4 | 4 | 3 | | 3 | 140 | 4 | 96 | | 4 | 4 | 4 | 64 |
| 12.7 | 7.0 | 15.1 | 9.2 | 16.0 | 12.8 | 15.4 | 10.5 | 14.2 | 15.0 | 14.5 | 9.4 | 7.0 | 11.9 |
| 2.3 | 3.4 | 3.9 | 2.8 | 1.4 | 2.6 | 1.6 | 2.5 | 1.9 | 0.8 | 1.9 | 3.5 | 3.7 | 0.7 |
| 4.5 | 4.7 | 2.9 | 1.8 | 1.6 | 2.4 | 1.4 | 2.1 | 3.1 | 1.8 | 1.7 | 2.5 | 2.9 | 0.5 |
| 132 | 5 | 2 | 4 | | 8 | 10 | 3 | 4 | | 4 | 1 | 1 | 91 |
| 16.0 | 11.1 | 3.4 | 2.6 | 3.0 | 3.8 | 2.8 | 3.0 | 1.8 | 2.0 | 3.8 | 2.2 | 3.8 | 0.4 |
| 37.0 | 11.0 | 26.0 | 22.9 | 3.6 | 13.5 | 7.8 | 23.3 | 2.3 | 1.1 | 1.0 | | 1.8 | 8.4 |
| 28 | 2 | | 12 | | | 33 | | 34 | | 39 | | 17 | 44 |
| 592 | 107 | 88 | 73 | 273 | 127 | 162 | 43 | 172 | 131 | 70 | 39 | 142 | 150 |
| 6.12 | 7.39 | 2.26 | 1.89 | 0.56 | 2.79 | 0.81 | 1.03 | 0.93 | 0.43 | 0.75 | 1.15 | 1.19 | 0.18 |
| 0.91 | 4.14 | 1.11 | 0.79 | 0.28 | 1.16 | 0.48 | 0.44 | 0.55 | 0.23 | 0.44 | 0.51 | 0.55 | 0.06 |
| 218 | 12 | 2 | 6 | | 68 | 260 | 11 | 253 | | 237 | 4 | 4 | 203 |
| 20 | 15 | 44 | 28 | 20 | 22 | 14 | 24 | 21 | 13 | 25 | 31 | 44 | 10 |
| 62 | 11 | 50 | 28 | | 44 | 65 | 59 | 79 | | 66 | 21 | 65 | 47 |
| 90 | 125 | 132 | 89 | 44 | 85 | 52 | 79 | 68 | 26 | 66 | 118 | 125 | 21 |
| 19.34 | 11.96 | 10.20 | 8.14 | 3.50 | 9.08 | 3.33 | 6.00 | 6.05 | 3.50 | 5.18 | 6.04 | 8.33 | 1.22 |
| 38.03 | 20.36 | 26.30 | 17.73 | 9.40 | 20.16 | 9.34 | 14.72 | 14.43 | 8.00 | 13.12 | 17.45 | 21.57 | 3.41 |
| 4.79 | 2.41 | 3.62 | 2.38 | 1.40 | 2.52 | 1.31 | 2.05 | 1.92 | 1.10 | 1.87 | 2.57 | 3.17 | 0.52 |
| 19.08 | 8.46 | 16.69 | 10.92 | 6.80 | 10.45 | 6.28 | 9.47 | 8.81 | 5.10 | 9.53 | 13.01 | 15.54 | 2.64 |
| 4.02 | 1.74 | 4.89 | 3.07 | 2.20 | 2.59 | 1.81 | 2.68 | 2.46 | 1.50 | 2.96 | 3.85 | 4.68 | 0.95 |
| 1.08 | 0.36 | 1.31 | 0.79 | 0.76 | 0.63 | 0.61 | 0.77 | 0.89 | 0.56 | 0.99 | 0.79 | 1.30 | 0.38 |
| 3.89 | 1.89 | 5.80 | 3.84 | 2.90 | 2.92 | 2.19 | 3.34 | 3.12 | 1.90 | 3.65 | 4.35 | 6.14 | 1.39 |
| 0.56 | 0.35 | 1.01 | 0.65 | 0.52 | 0.50 | 0.37 | 0.58 | 0.53 | 0.35 | 0.61 | 0.72 | 1.06 | 0.25 |
| 3.49 | 2.21 | 6.85 | 4.38 | 3.20 | 3.42 | 2.37 | 3.93 | 3.55 | 2.20 | 4.15 | 4.89 | 7.09 | 1.76 |
| 0.72 | 0.52 | 1.49 | 0.96 | 0.68 | 0.76 | 0.51 | 0.85 | 0.76 | 0.46 | 0.90 | 1.07 | 1.53 | 0.39 |
| 2.06 | 1.70 | 4.58 | 2.96 | 1.90 | 2.36 | 1.54 | 2.61 | 2.27 | 1.30 | 2.74 | 3.37 | 4.48 | 1.13 |
| 0.31 | 0.28 | 0.69 | 0.46 | 0.30 | 0.37 | 0.23 | 0.39 | 0.34 | 0.22 | 0.40 | 0.51 | 0.65 | 0.17 |
| 2.05 | 2.04 | 4.67 | 3.10 | 2.00 | 2.58 | 1.56 | 2.62 | 2.27 | 1.30 | 2.72 | 3.53 | 4.20 | 1.14 |
| 0.32 | 0.35 | 0.73 | 0.50 | 0.32 | 0.42 | 0.25 | 0.40 | 0.35 | 0.22 | 0.42 | 0.54 | 0.64 | 0.17 |

| **Sample** | **RAX06 A034** | **RAX06 A035** | **RAX06 A036A** | **RAX06 A036B** | **RAX06 A037** | **RAX06 A041** | **RAX06 A105** | **RAX06 A109** | **RAX06 A112** | **RAX06 A114** | **RAX06 A119** | **RAX06 A121** |
|---|---|---|---|---|---|---|---|---|---|---|---|---|
| Easting | 539252 | 537889 | 538038 | 538038 | 538335 | 537001 | 531043 | 531796 | 532315 | 532289 | 533826 | 533139 |
| Northing | 5414700 | 5413141 | 5413191 | 5413191 | 5413270 | 5411195 | 5409506 | 5411651 | 5412377 | 5413843 | 5409695 | 5409284 |
| geochem. Type* | IAT/BAB | TRD | IAT/BAB | TRD | IAT/BAB | CAB | CAB gabbro | TRD | TRD | IAT/BAB | CAB | CAB |
| strat. unit | MM | MM | MM | MM | MM | RILG | RILG | MM | MM | MM | RILG | RILG |
| | | | | | | | | | | | | |
| $SiO_2$ | 51.78 | 71.86 | 38.11 | 74.30 | 39.84 | 45.07 | 50.23 | 76.13 | 74.00 | 53.28 | 48.43 | 48.21 |
| $TiO_2$ | 0.71 | 0.33 | 0.65 | 0.31 | 0.67 | 0.61 | 0.95 | 0.23 | 0.21 | 0.41 | 1.11 | 1.33 |
| $Al_2O_3$ | 17.16 | 12.11 | 13.07 | 12.76 | 13.07 | 13.24 | 16.39 | 12.61 | 12.30 | 17.87 | 16.38 | 17.37 |
| MnO | 0.17 | 0.22 | 0.19 | 0.07 | 0.15 | 0.17 | 0.16 | 0.03 | 0.09 | 0.59 | 0.15 | 0.18 |
| Mgo | 5.21 | 2.21 | 4.59 | 0.70 | 4.13 | 7.65 | 6.05 | 0.66 | 0.48 | 4.40 | 6.29 | 6.91 |
| CaO | 3.04 | 0.85 | 15.29 | 0.33 | 14.54 | 11.70 | 8.81 | 0.30 | 2.47 | 2.86 | 8.19 | 6.45 |
| $Na_2O$ | 4.68 | 3.64 | 4.39 | 6.35 | 4.62 | 4.61 | 4.25 | 6.65 | 3.20 | 6.20 | 2.39 | 2.93 |
| $K_2O$ | 0.14 | 0.47 | 0.08 | 0.27 | 0.06 | 0.16 | 0.67 | 0.10 | 1.52 | 0.08 | 1.80 | 2.94 |
| $P_2O_5$ | 0.14 | 0.08 | 0.08 | 0.07 | 0.07 | 0.12 | 0.21 | 0.04 | 0.03 | 0.06 | 0.20 | 0.25 |
| LOI | 3.81 | 2.90 | 16.09 | 0.93 | 15.62 | 7.59 | 3.24 | 0.74 | 3.00 | 3.76 | 7.30 | 4.60 |
| $Fe_2O_3t$ | 13.51 | 5.34 | 7.57 | 3.84 | 7.27 | 8.70 | 9.29 | 2.33 | 2.90 | 10.40 | 7.90 | 9.15 |
| Total | 100.39 | 100.00 | 100.19 | 99.94 | 100.11 | 99.77 | 100.29 | 99.82 | 100.00 | 99.95 | 100.19 | 100.38 |
| | | | | | | | | | | | | |
| Ba | 48 | 63 | 24 | 25 | 26 | 88 | 250 | 46 | 136 | 29 | 337 | 340 |
| Cr | | | 325 | 21 | 286 | 400 | 57 | | | 17 | 115 | 72 |
| Cs | 0.07 | 0.15 | 0.12 | 0.09 | 0.06 | 0.25 | 0.11 | 0.03 | 0.30 | 0.06 | 0.83 | 1.04 |
| Cu | 121 | 13 | 90 | 3 | 100 | 71 | 77 | 35 | | 140 | 58 | 99 |
| Ga | 14.8 | 14.1 | 9.5 | 14.1 | 10.6 | 8.8 | 14.0 | 10.5 | 16.0 | 12.2 | 14.9 | 15.6 |
| Hf | 1.9 | 3.0 | 1.0 | 5.0 | 1.0 | 1.2 | 2.5 | 3.7 | 4.0 | 1.0 | 4.3 | 4.0 |
| Nb | 1.5 | 2.0 | 0.5 | 3.7 | 0.5 | 2.0 | 3.3 | 2.8 | 3.6 | 0.8 | 6.9 | 6.3 |
| Ni | 10 | 1 | 73 | 4 | 89 | 263 | 35 | 2 | | 12 | 38 | 36 |
| Pb | 1.6 | 40.0 | 1.2 | 2.3 | 1.0 | 2.9 | 2.2 | 3.2 | 2.0 | 5.5 | 8.2 | 3.5 |
| Rb | 2.7 | 5.1 | 1.3 | 4.1 | | 3.2 | 9.5 | 1.1 | 18.0 | | 25.7 | 48.4 |
| Sc | 44 | 10 | 26 | 17 | 24 | 25 | 29 | | | 32 | 34 | 29 |
| Sr | 135 | 65 | 112 | 53 | 121 | 211 | 221 | 62 | 60 | 125 | 294 | 218 |
| Th | 1.05 | 1.66 | 0.11 | 1.33 | 0.11 | 1.92 | 3.96 | 2.78 | 1.30 | 0.48 | 4.81 | 5.06 |
| U | 0.55 | 0.53 | 0.50 | 0.70 | 0.34 | 0.62 | 0.81 | 0.97 | 0.57 | 0.20 | 1.08 | 2.01 |
| V | 300 | 2 | 170 | 1 | 163 | 237 | 254 | 15 | | 266 | 270 | 300 |
| Y | 21 | 39 | 17 | 45 | 13 | 14 | 22 | 34 | 43 | 9 | 21 | 27 |
| Zn | 99 | 150 | 51 | 79 | 47 | 51 | 56 | 18 | | 129 | 55 | 70 |
| Zr | 63 | 98 | 34 | 177 | 34 | 47 | 99 | 127 | 148 | 32 | 168 | 158 |
| | | | | | | | | | | | | |
| La | 5.92 | 8.22 | 1.20 | 8.33 | 1.12 | 8.08 | 14.94 | 12.80 | 7.80 | 2.48 | 17.87 | 19.82 |
| Ce | 14.90 | 20.23 | 3.84 | 22.08 | 3.64 | 17.86 | 33.10 | 28.64 | 20.00 | 6.36 | 40.91 | 45.23 |
| Pr | 2.07 | 2.83 | 0.70 | 3.25 | 0.65 | 2.27 | 4.28 | 3.63 | 2.90 | 0.84 | 5.07 | 5.72 |
| Nd | 9.74 | 13.69 | 3.97 | 16.20 | 3.68 | 9.64 | 18.13 | 15.50 | 14.00 | 3.98 | 20.62 | 23.66 |
| Sm | 2.74 | 4.08 | 1.59 | 5.07 | 1.36 | 2.31 | 4.13 | 4.02 | 4.30 | 1.23 | 4.36 | 5.21 |
| Eu | 0.88 | 1.12 | 0.60 | 1.28 | 0.40 | 0.73 | 1.27 | 0.79 | 1.10 | 0.41 | 1.28 | 1.55 |
| Gd | 3.30 | 5.16 | 2.34 | 6.36 | 1.93 | 2.43 | 4.12 | 4.66 | 5.40 | 1.49 | 4.08 | 5.19 |
| Tb | 0.55 | 0.90 | 0.42 | 1.10 | 0.33 | 0.38 | 0.62 | 0.81 | 0.96 | 0.25 | 0.63 | 0.80 |
| Dy | 3.62 | 6.14 | 2.89 | 7.47 | 2.22 | 2.42 | 3.85 | 5.61 | 6.20 | 1.64 | 4.01 | 4.99 |
| Ho | 0.79 | 1.36 | 0.62 | 1.65 | 0.49 | 0.50 | 0.78 | 1.25 | 1.40 | 0.35 | 0.81 | 1.03 |
| Er | 2.40 | 4.07 | 1.84 | 5.05 | 1.46 | 1.44 | 2.23 | 3.82 | 4.40 | 1.03 | 2.35 | 2.92 |
| Tm | 0.36 | 0.62 | 0.27 | 0.77 | 0.22 | 0.21 | 0.32 | 0.59 | 0.74 | 0.15 | 0.34 | 0.42 |
| Yb | 2.38 | 4.21 | 1.76 | 5.23 | 1.49 | 1.35 | 2.12 | 4.02 | 4.90 | 1.06 | 2.20 | 2.77 |
| Lu | 0.37 | 0.66 | 0.27 | 0.82 | 0.23 | 0.21 | 0.32 | 0.64 | 0.84 | 0.17 | 0.33 | 0.41 |

| RAX06 A126 | RAX06 A127 | RAX06 A128 | RAX06 A130 | RAX06 A158b | RAX06 A162 | RAX06 A164 | RAX06 A165 | RAX06 A166 | RAX06 A167 | RAX06 A169A | RAX06 A169B | RAX06 A170 | RAX06 A177 |
|---|---|---|---|---|---|---|---|---|---|---|---|---|---|
| 535206 | 534822 | 534614 | 533712 | 544201 | 543911 | 543428 | 542902 | 542852 | 542430 | 541703 | 541703 | 541306 | 541667 |
| 5409987 | 5409499 | 5409319 | 5408793 | 5421245 | 5420255 | 5419903 | 5419374 | 5419254 | 5418372 | 5418157 | 5418157 | 5416919 | 5412763 |
| CARD | CARD | CARD | CAB | IAT/BAB | EMORB | EMORB | EMORB | EMORB | CAB Gabbro | CARD tuff | CAB Gabbro | IAT/BAB | CARD |
| RILG | RILG | RILG | RILG | MM | HR | HR | HR | HR | MM | MM | MM | MM | RILG |
| 63.30 | 70.00 | 60.97 | 51.60 | 49.90 | 48.80 | 48.06 | 48.48 | 49.20 | 51.20 | 70.38 | 50.14 | 45.99 | 70.40 |
| 0.77 | 0.52 | 0.65 | 0.78 | 0.44 | 1.69 | 1.26 | 2.16 | 2.64 | 0.90 | 0.37 | 0.81 | 0.90 | 0.40 |
| 16.93 | 14.30 | 16.27 | 14.69 | 19.29 | 16.90 | 15.99 | 14.37 | 14.40 | 16.40 | 14.38 | 17.47 | 15.42 | 14.00 |
| 0.13 | 0.05 | 0.16 | 0.12 | 0.14 | 0.19 | 0.20 | 0.20 | 0.21 | 0.16 | 0.07 | 0.16 | 0.17 | 0.24 |
| 1.82 | 0.88 | 1.90 | 3.36 | 6.67 | 7.43 | 8.01 | 6.58 | 5.73 | 6.19 | 1.52 | 7.51 | 5.67 | 1.24 |
| 2.92 | 1.48 | 4.74 | 10.01 | 9.33 | 8.40 | 11.15 | 10.16 | 7.95 | 11.21 | 2.83 | 10.98 | 15.99 | 0.32 |
| 3.23 | 4.30 | 2.66 | 5.43 | 2.89 | 3.40 | 3.19 | 3.80 | 4.80 | 1.80 | 4.86 | 2.41 | 1.54 | 5.50 |
| 3.24 | 4.06 | 2.87 | 2.52 | 1.46 | 0.64 | 0.17 | 0.44 | 0.33 | 0.67 | 0.99 | 1.15 | 0.99 | 2.18 |
| 0.17 | 0.15 | 0.24 | 0.23 | 0.05 | 0.21 | 0.14 | 0.24 | 0.30 | 0.14 | 0.09 | 0.17 | 0.11 | 0.08 |
| 2.46 | 1.00 | 3.24 | 5.70 | 1.85 | 1.40 | 1.01 | 0.83 | 1.40 | 0.40 | 0.86 | 0.75 | 3.57 | 1.20 |
| 4.81 | 2.70 | 6.43 | 5.50 | 8.35 | 10.80 | 11.52 | 13.22 | 13.70 | 10.60 | 3.76 | 9.10 | 9.76 | 3.40 |
| 99.79 | 99.60 | 100.15 | 100.00 | 100.42 | 99.70 | 100.76 | 100.55 | 100.50 | 99.50 | 100.12 | 100.71 | 100.18 | 99.10 |
| 1032 | 1390 | 880 | 1094 | 312 | 180 | 33 | 70 | 120 | 386 | 639 | 327 | 97 | 797 |
| | | 18 | 225 | 119 | | 247 | 178 | | | 26 | 204 | 194 | |
| 2.57 | 0.44 | 2.19 | 0.45 | 3.78 | 0.90 | 0.31 | 0.28 | 0.14 | 0.61 | 0.77 | 1.04 | 0.48 | 0.36 |
| 8 | | 31 | 55 | 51 | | 78 | 68 | | | 12 | 38 | 12 | |
| 17.3 | 13.0 | 14.9 | 10.6 | 14.6 | 19.0 | 15.3 | 15.9 | 20.0 | 16.0 | 11.6 | 14.3 | 13.1 | 13.0 |
| 6.5 | 4.2 | 3.6 | 2.7 | 0.8 | 3.1 | 2.3 | 3.9 | 4.0 | 1.4 | 2.2 | 2.4 | 1.2 | 3.8 |
| 13.5 | 6.6 | 3.8 | 4.6 | 0.8 | 4.8 | 2.1 | 3.4 | 6.5 | 2.1 | 4.5 | 3.2 | 1.5 | 6.9 |
| 2 | | 4 | 37 | 40 | | 79 | 46 | | | 8 | 63 | 66 | |
| 12.1 | 18.0 | 12.7 | 5.2 | 19.0 | 3.0 | 1.1 | 1.3 | 3.0 | 7.0 | 3.7 | 2.4 | 26.2 | 5.0 |
| 127.7 | 78.0 | 63.7 | 35.2 | 53.8 | 15.0 | 3.7 | 5.9 | 4.7 | 13.0 | 22.0 | 27.7 | 18.1 | 31.0 |
| | | 13 | 28 | 26 | | 34 | 42 | | | 14 | 44 | 36 | |
| 345 | 239 | 443 | 185 | 243 | 373 | 257 | 318 | 140 | 318 | 212 | 251 | 277 | 121 |
| 15.02 | 11.00 | 5.23 | 6.26 | 0.28 | 1.20 | 0.23 | 0.30 | 0.53 | 2.80 | 5.87 | 2.90 | 0.58 | 7.10 |
| 3.93 | 2.90 | 2.04 | 1.59 | 0.12 | 0.35 | 0.12 | 0.17 | 0.27 | 0.67 | 1.45 | 0.63 | 0.43 | 1.40 |
| 46 | | 67 | 162 | 194 | | 270 | 300 | | | 56 | 230 | 291 | |
| 46 | 24 | 34 | 22 | 11 | 33 | 23 | 35 | 46 | 20 | 16 | 18 | 18 | 16 |
| 65 | | 69 | 43 | 28 | | 86 | 71 | | | 24 | 46 | 66 | |
| 260 | 166 | 136 | 109 | 29 | 148 | 93 | 168 | 201 | 56 | 82 | 93 | 44 | 126 |
| 39.20 | 28.00 | 21.00 | 18.68 | 2.00 | 12.00 | 4.02 | 6.43 | 9.40 | 12.00 | 16.69 | 11.92 | 3.73 | 21.00 |
| 80.46 | 52.00 | 43.18 | 39.04 | 5.31 | 31.00 | 11.80 | 20.01 | 29.00 | 25.00 | 32.81 | 26.68 | 9.48 | 43.00 |
| 9.85 | 5.80 | 5.35 | 4.86 | 0.77 | 4.30 | 1.79 | 3.21 | 4.50 | 3.10 | 3.54 | 3.42 | 1.36 | 4.60 |
| 39.47 | 22.00 | 22.36 | 19.63 | 3.82 | 20.00 | 9.36 | 16.41 | 22.00 | 13.00 | 13.56 | 14.53 | 6.79 | 17.00 |
| 8.17 | 4.20 | 5.16 | 4.26 | 1.26 | 5.00 | 2.86 | 4.79 | 6.50 | 3.30 | 2.71 | 3.36 | 2.16 | 3.20 |
| 1.92 | 1.10 | 1.41 | 1.21 | 0.50 | 1.60 | 1.13 | 1.76 | 2.30 | 1.10 | 0.87 | 1.03 | 0.82 | 0.78 |
| 7.47 | 4.00 | 5.34 | 4.14 | 1.67 | 5.70 | 3.66 | 5.80 | 7.90 | 3.60 | 2.57 | 3.40 | 2.82 | 2.90 |
| 1.16 | 0.63 | 0.85 | 0.63 | 0.29 | 0.94 | 0.63 | 0.98 | 1.40 | 0.57 | 0.41 | 0.53 | 0.48 | 0.43 |
| 7.35 | 3.70 | 5.52 | 3.94 | 1.94 | 5.60 | 4.17 | 6.33 | 7.90 | 3.30 | 2.60 | 3.37 | 3.24 | 2.40 |
| 1.54 | 0.75 | 1.16 | 0.79 | 0.42 | 1.20 | 0.87 | 1.31 | 1.60 | 0.70 | 0.55 | 0.69 | 0.69 | 0.51 |
| 4.64 | 2.20 | 3.53 | 2.31 | 1.27 | 3.10 | 2.53 | 3.81 | 4.40 | 2.00 | 1.67 | 2.01 | 2.02 | 1.60 |
| 0.70 | 0.39 | 0.54 | 0.34 | 0.18 | 0.47 | 0.36 | 0.53 | 0.67 | 0.30 | 0.26 | 0.29 | 0.29 | 0.28 |
| 4.76 | 2.50 | 3.63 | 2.26 | 1.20 | 3.00 | 2.29 | 3.38 | 4.10 | 2.00 | 1.73 | 1.84 | 1.87 | 2.00 |
| 0.74 | 0.42 | 0.58 | 0.34 | 0.19 | 0.51 | 0.35 | 0.50 | 0.65 | 0.33 | 0.27 | 0.28 | 0.28 | 0.35 |

| **Sample** | **RAX07 A008** | **RAX07 A030** | **RAX07 A031** | **RAX07 A032** | **RAX07 A033B** | **RAX07 A061a** | **RAX07 A061b** | **RAX07 A062a** | **RAX07 A062b** | **RAX07 A064** | **RAX07 A065** | **RAX07 A069** |
|---|---|---|---|---|---|---|---|---|---|---|---|---|
| Easting | 536355 | 532336 | 532386 | 532270 | 532175 | 540116 | 540116 | 539991 | 539991 | 540101 | 540128 | 540558 |
| Northing | 5413477 | 5406847 | 5407004 | 5407408 | 5407818 | 5417195 | 5417195 | 5416791 | 5416791 | 5416272 | 5416170 | 5415116 |
| geochem. Type* | TRD | CAB | CAB | CAB | CAB | TRD | CAB diabase | TRD | WPB | TRD | CAB | IAT/BAB |
| strat. unit | MM | RILG | RILG | RILG | RILG | MM | MM | MM | | MM | MM | MM |
| $SiO_2$ | 76.70 | 63.20 | 65.90 | 48.70 | 43.50 | 81.70 | 46.20 | 67.20 | 46.80 | 70.50 | 47.20 | 50.20 |
| $TiO_2$ | 0.26 | 0.58 | 0.79 | 0.88 | 0.79 | 0.15 | 0.78 | 0.33 | 2.79 | 0.35 | 1.25 | 0.72 |
| $Al_2O_3$ | 12.20 | 14.20 | 12.70 | 17.90 | 14.90 | 9.90 | 19.50 | 15.70 | 15.20 | 15.30 | 15.40 | 17.20 |
| MnO | 0.06 | 0.16 | 0.16 | 0.20 | 0.11 | 0.03 | 0.36 | 0.06 | 0.26 | 0.03 | 0.27 | 0.18 |
| MgO | 0.23 | 3.48 | 2.67 | 8.89 | 4.44 | 0.06 | 6.76 | 2.65 | 7.16 | 0.74 | 6.94 | 5.17 |
| CaO | 1.45 | 2.80 | 3.12 | 6.85 | 13.22 | 0.24 | 8.01 | 1.68 | 9.98 | 1.60 | 8.32 | 6.99 |
| $Na_2O$ | 4.50 | 2.10 | 1.70 | 3.60 | 3.50 | 5.00 | 2.40 | 3.20 | 2.60 | 4.40 | 3.50 | 5.80 |
| $K_2O$ | 1.49 | 2.48 | 2.61 | 0.44 | 1.57 | 1.22 | 1.63 | 2.35 | 0.61 | 2.02 | 0.44 | 0.14 |
| $P_2O_5$ | 0.05 | 0.16 | 0.23 | 0.18 | 0.22 | 0.02 | 0.12 | 0.06 | 0.36 | 0.07 | 0.40 | 0.09 |
| LOI | 2.00 | 2.80 | 2.80 | 4.50 | 9.60 | 0.10 | 3.00 | 1.80 | 1.10 | 1.40 | 2.30 | 5.30 |
| $Fe_2O_3t$ | 1.40 | 8.80 | 7.50 | 8.20 | 8.70 | 1.70 | 11.00 | 5.10 | 14.20 | 3.50 | 14.50 | 8.40 |
| Total | 99.70 | 98.20 | 97.90 | 96.40 | 98.50 | 100.10 | 97.00 | 98.60 | 100.30 | 98.80 | 98.60 | 97.80 |
| Ba | 88 | 823 | 979 | 389 | 334 | 278 | 560 | 139 | 168 | 228 | 571 | 55 |
| Cr | | | | 359 | | | 69 | | 81 | | 168 | 29 |
| Cs | 0.14 | 1.20 | 1.50 | 0.96 | 3.00 | 0.07 | 0.85 | 1.40 | 1.20 | 0.88 | 0.30 | 0.34 |
| Cu | | 155 | 46 | 132 | 35 | | 97 | | 89 | | 48 | 43 |
| Ga | 15.0 | 17.0 | 14.0 | 22.0 | 15.0 | 14.0 | 21.0 | 19.0 | 22.0 | 22.0 | 17.0 | 19.0 |
| Hf | 4.6 | 1.1 | 2.0 | 3.7 | 2.3 | 4.4 | 1.2 | 3.7 | 3.9 | 4.0 | 1.7 | 1.5 |
| Nb | 3.9 | 1.6 | 2.4 | 5.8 | 4.2 | 3.1 | 1.8 | 2.9 | 8.5 | 3.1 | 3.1 | 2.4 |
| Ni | | 12 | | 123 | 195 | | 15 | | 90 | | 60 | 14 |
| Pb | 2.0 | 5.0 | 7.0 | 6.0 | 5.0 | 4.0 | 7.0 | 7.0 | 3.0 | 20.0 | 6.0 | 4.0 |
| Rb | 11.0 | 65.0 | 54.0 | 10.0 | 41.0 | 11.0 | 26.0 | 36.0 | 11.0 | 42.0 | 7.7 | 1.9 |
| Sc | 9 | 29 | 18 | 31 | 32 | 7 | 43 | 15 | 31 | 17 | 40 | 34 |
| Sr | 68 | 168 | 188 | 364 | 287 | 61 | 285 | 150 | 356 | 159 | 287 | 209 |
| Th | 1.30 | 1.60 | 2.20 | 7.10 | 5.00 | 3.50 | 2.20 | 2.10 | 0.54 | 2.40 | 3.60 | 0.48 |
| U | 0.84 | 0.52 | 0.73 | 1.70 | 0.41 | 1.00 | 0.48 | 0.70 | 0.20 | 1.00 | 0.91 | 0.30 |
| V | 6 | 248 | 183 | 233 | 134 | | 333 | 18 | 329 | 31 | 428 | 270 |
| Y | 45 | 16 | 25 | 27 | 20 | 49 | 17 | 33 | 30 | 30 | 24 | 20 |
| Zn | 63 | 91 | 80 | 87 | 97 | 25 | 119 | 106 | 164 | 258 | 139 | 104 |
| Zr | 160 | 36 | 70 | 128 | 84 | 126 | 34 | 119 | 151 | 123 | 51 | 46 |
| La | 6.30 | 8.50 | 10.00 | 20.00 | 15.00 | 16.00 | 10.00 | 8.90 | 11.00 | 12.00 | 16.00 | 3.90 |
| Ce | 19.00 | 17.00 | 23.00 | 44.00 | 36.00 | 36.00 | 24.00 | 20.00 | 29.00 | 28.00 | 34.00 | 9.60 |
| Pr | 3.00 | 2.20 | 3.00 | 5.20 | 4.60 | 4.80 | 3.00 | 2.80 | 4.20 | 3.80 | 4.60 | 1.40 |
| Nd | 15.00 | 9.80 | 14.00 | 21.00 | 20.00 | 21.00 | 13.00 | 13.00 | 21.00 | 16.00 | 19.00 | 7.30 |
| Sm | 4.80 | 2.50 | 3.50 | 4.50 | 4.50 | 5.60 | 3.10 | 3.70 | 5.70 | 4.30 | 4.30 | 2.20 |
| Eu | 1.20 | 0.78 | 1.00 | 1.40 | 1.20 | 1.20 | 0.93 | 1.10 | 2.30 | 1.30 | 1.40 | 0.77 |
| Gd | 6.10 | 2.90 | 4.10 | 4.70 | 4.10 | 7.30 | 3.30 | 4.90 | 6.80 | 5.20 | 4.70 | 3.00 |
| Tb | 1.10 | 0.43 | 0.65 | 0.71 | 0.64 | 1.30 | 0.52 | 0.88 | 1.10 | 0.88 | 0.74 | 0.53 |
| Dy | 7.30 | 2.70 | 4.00 | 4.50 | 3.50 | 8.00 | 3.00 | 5.50 | 5.90 | 5.40 | 4.20 | 3.30 |
| Ho | 1.60 | 0.57 | 0.88 | 0.91 | 0.74 | 1.70 | 0.64 | 1.20 | 1.20 | 1.10 | 0.88 | 0.74 |
| Er | 4.50 | 1.60 | 2.40 | 2.50 | 2.00 | 4.90 | 1.70 | 3.40 | 3.10 | 3.20 | 2.40 | 2.00 |
| Tm | 0.75 | 0.24 | 0.39 | 0.40 | 0.30 | 0.81 | 0.24 | 0.55 | 0.43 | 0.48 | 0.36 | 0.30 |
| Yb | 5.30 | 1.70 | 2.70 | 2.80 | 2.00 | 5.60 | 1.70 | 3.90 | 2.90 | 3.20 | 2.30 | 2.10 |
| Lu | 0.80 | 0.26 | 0.42 | 0.43 | 0.33 | 0.93 | 0.26 | 0.64 | 0.44 | 0.51 | 0.35 | 0.33 |

| RAX07 A070 | RAX07 A071 | RAX07 A072 | RAX07 A073 | RAX07 A075a | RAX07 A075b | RAX07 A076b | RAX07 A095 | RAX07 A096 | RAX07 A102A | RAX07 A103 | RAX07 A106 | RAX07 A109 | RAX07 A110 |
|---|---|---|---|---|---|---|---|---|---|---|---|---|---|
| 540512 | 541731 | 542192 | 541184 | 541440 | 541440 | 541778 | 536971 | 537220 | 536057 | 535430 | 533145 | 533711 | 533907 |
| 5415564 | 5414301 | 5413478 | 5412626 | 5418710 | 5418710 | 5418731 | 5411163 | 5411714 | 5410073 | 5410108 | 5409281 | 5414513 | 5414575 |
| IAT/BAB | CARD | CARD | CARD | TRD | IAT/BAB | TRD | CAB | CAB | CAB | CARD | CAB | IAT/BAB | IAT/BAB |
| MM | RILG | RILG | RILG | MM | MM | MM | RILG | RILG | RILG | RILG | RILG | MM | MM |
| 47.40 | 69.30 | 70.60 | 71.00 | 77.60 | 51.10 | 70.50 | 44.50 | 47.60 | 45.60 | 67.70 | 49.00 | 50.20 | 52.60 |
| 0.67 | 0.52 | 0.48 | 0.34 | 0.23 | 0.41 | 0.36 | 0.60 | 1.09 | 0.58 | 0.58 | 1.35 | 0.44 | 0.40 |
| 16.00 | 14.60 | 13.50 | 12.90 | 11.30 | 17.80 | 13.80 | 13.60 | 15.90 | 12.30 | 15.10 | 17.00 | 16.50 | 17.70 |
| 0.19 | 0.08 | 0.06 | 0.05 | 0.04 | 0.13 | 0.05 | 0.15 | 0.12 | 0.22 | 0.11 | 0.18 | 0.26 | 0.20 |
| 5.49 | 1.28 | 1.00 | 0.92 | 2.07 | 6.49 | 1.49 | 7.39 | 7.17 | 6.01 | 0.93 | 6.93 | 6.31 | 5.62 |
| 7.55 | 1.30 | 1.09 | 2.34 | 0.38 | 7.21 | 2.43 | 11.57 | 9.05 | 11.67 | 1.52 | 6.74 | 9.82 | 7.83 |
| 6.10 | 5.60 | 4.10 | 4.80 | 2.40 | 4.80 | 6.00 | 4.90 | 3.80 | 3.10 | 2.10 | 2.40 | 3.70 | 5.10 |
| 0.13 | 1.64 | 4.08 | 2.22 | 2.19 | 0.22 | 0.56 | 0.13 | 0.64 | 0.67 | 5.86 | 3.09 | 0.04 | 0.06 |
| 0.11 | 0.10 | 0.11 | 0.08 | 0.02 | 0.08 | 0.09 | 0.12 | 0.18 | 0.17 | 0.11 | 0.24 | 0.04 | 0.04 |
| 7.60 | 1.30 | 1.70 | 2.50 | 1.40 | 2.00 | 0.70 | 9.40 | 6.10 | 11.70 | 2.10 | 3.80 | 1.60 | 1.80 |
| 8.90 | 3.70 | 2.90 | 2.80 | 1.80 | 10.10 | 3.70 | 7.90 | 8.30 | 7.50 | 3.50 | 9.10 | 10.50 | 8.90 |
| 97.70 | 98.40 | 98.80 | 99.20 | 98.20 | 98.50 | 99.10 | 97.60 | 96.70 | 97.00 | 98.30 | 96.70 | 98.00 | 98.50 |
| 74 | 961 | 1400 | 657 | 223 | 77 | 127 | 82 | 164 | 389 | 1420 | 371 | 47 | 53 |
| 27 | | | | | 15 | | 454 | 322 | 400 | | 74 | 62 | 54 |
| 0.30 | 0.24 | 0.37 | 0.73 | 0.52 | 0.09 | 0.05 | 0.32 | 0.49 | 0.19 | 2.10 | 1.10 | | 0.03 |
| 31 | | 52 | | | 51 | 15 | 66 | 61 | 14 | | 102 | | 18 |
| 14.0 | 14.0 | 14.0 | 12.0 | 13.0 | 17.0 | 14.0 | 12.0 | 15.0 | 12.0 | 18.0 | 20.0 | 17.0 | 13.0 |
| 1.2 | 5.5 | 4.9 | 4.3 | 3.3 | 0.8 | 2.0 | 1.3 | 2.4 | 1.3 | 6.3 | 4.2 | 0.7 | 0.7 |
| 2.2 | 5.8 | 6.0 | 5.7 | 2.6 | 4.7 | 1.9 | 2.3 | 3.8 | 2.5 | 15.0 | 7.2 | 1.0 | 1.2 |
| 20 | | | | | 15 | | 166 | 139 | 149 | | 31 | 37 | 28 |
| 2.0 | 20.0 | 6.0 | 10.0 | 6.0 | 2.0 | 2.0 | 4.0 | 2.0 | 3.0 | 17.0 | 3.0 | 5.0 | 3.0 |
| 1.6 | 40.0 | 51.0 | 45.0 | 29.0 | 2.1 | 7.9 | 2.1 | 11.0 | 21.0 | 236.0 | 59.0 | 0.2 | 0.3 |
| 32 | 9 | 8 | 9 | 9 | 38 | 16 | 31 | 33 | 31 | 7 | 36 | 37 | 35 |
| 165 | 291 | 98 | 158 | 60 | 276 | 204 | 173 | 241 | 114 | 391 | 285 | 231 | 201 |
| 0.45 | 11.00 | 8.70 | 6.10 | 1.70 | 0.88 | 0.95 | 1.90 | 2.50 | 3.10 | 15.00 | 5.20 | 0.46 | 0.66 |
| 0.46 | 2.50 | 2.70 | 1.60 | 0.79 | 0.27 | 0.46 | 0.51 | 0.52 | 0.94 | 3.90 | 1.30 | 0.21 | 0.23 |
| 261 | 51 | 42 | 33 | 7 | 249 | 35 | 236 | 260 | 211 | 10 | 344 | 264 | 228 |
| 19 | 31 | 29 | 23 | 22 | 9 | 20 | 14 | 21 | 14 | 39 | 28 | 9 | 8 |
| 101 | 51 | 38 | 40 | 49 | 84 | 38 | 95 | 106 | 122 | 68 | 106 | 127 | 114 |
| 38 | 184 | 163 | 150 | 98 | 23 | 64 | 45 | 91 | 52 | 224 | 140 | 21 | 24 |
| 3.50 | 28.00 | 24.00 | 19.00 | 6.90 | 6.10 | 5.00 | 8.70 | 12.00 | 11.00 | 42.00 | 22.00 | 2.80 | 2.80 |
| 8.80 | 53.00 | 45.00 | 37.00 | 16.00 | 13.00 | 12.00 | 18.00 | 27.00 | 23.00 | 87.00 | 49.00 | 6.60 | 6.60 |
| 1.30 | 6.10 | 5.40 | 4.30 | 2.20 | 1.70 | 1.70 | 2.40 | 3.80 | 2.70 | 11.00 | 6.20 | 0.89 | 0.86 |
| 6.40 | 23.00 | 22.00 | 17.00 | 9.60 | 7.00 | 7.60 | 9.90 | 17.00 | 12.00 | 42.00 | 27.00 | 4.30 | 4.10 |
| 2.00 | 4.70 | 4.60 | 3.40 | 2.50 | 1.60 | 2.20 | 2.20 | 4.00 | 2.70 | 8.30 | 6.00 | 1.30 | 1.10 |
| 0.68 | 1.20 | 1.30 | 0.87 | 0.45 | 0.56 | 0.69 | 0.74 | 1.20 | 0.83 | 2.10 | 1.60 | 0.45 | 0.39 |
| 2.70 | 4.90 | 4.70 | 3.50 | 2.70 | 1.80 | 2.90 | 2.50 | 4.10 | 2.80 | 7.50 | 5.70 | 1.40 | 1.30 |
| 0.48 | 0.81 | 0.81 | 0.59 | 0.50 | 0.29 | 0.52 | 0.41 | 0.67 | 0.41 | 1.10 | 0.89 | 0.24 | 0.22 |
| 3.00 | 4.90 | 4.70 | 3.50 | 3.30 | 1.60 | 3.20 | 2.40 | 3.80 | 2.40 | 6.60 | 5.30 | 1.60 | 1.50 |
| 0.67 | 1.00 | 1.00 | 0.77 | 0.76 | 0.34 | 0.69 | 0.49 | 0.79 | 0.51 | 1.40 | 1.10 | 0.34 | 0.31 |
| 1.90 | 3.00 | 2.90 | 2.20 | 2.30 | 0.96 | 2.00 | 1.40 | 2.10 | 1.40 | 4.00 | 3.00 | 0.94 | 0.87 |
| 0.29 | 0.49 | 0.48 | 0.37 | 0.40 | 0.15 | 0.32 | 0.21 | 0.32 | 0.21 | 0.62 | 0.45 | 0.15 | 0.14 |
| 1.90 | 3.50 | 3.40 | 2.60 | 3.00 | 0.93 | 2.20 | 1.40 | 2.10 | 1.50 | 4.30 | 3.00 | 1.00 | 0.88 |
| 0.31 | 0.58 | 0.58 | 0.43 | 0.51 | 0.16 | 0.35 | 0.22 | 0.35 | 0.23 | 0.68 | 0.45 | 0.15 | 0.14 |

| **Sample** | **RAX07 A111** | **RAX07 A195** | **RAX07 A197** | **RAX07 A198** |
|---|---|---|---|---|
| Easting | 533898 | 538135 | 531618 | 530882 |
| Northing | 5414509 | 5410802 | 5407870 | 5407271 |
| geochem. Type* | CAB gabbro | CARD | CAB | CAB |
| strat. unit | MM | RILG | RILG | RILG |
| | | | | |
| $SiO_2$ | 54.10 | 70.20 | 51.90 | 50.10 |
| $TiO_2$ | 0.53 | 0.46 | 0.94 | 0.83 |
| $Al_2O_3$ | 17.00 | 14.90 | 17.40 | 16.70 |
| MnO | 0.24 | 0.05 | 0.16 | 0.16 |
| MgO | 4.78 | 0.91 | 5.02 | 6.66 |
| CaO | 5.98 | 2.65 | 7.32 | 9.39 |
| $Na_2O$ | 4.10 | 3.80 | 4.10 | 2.10 |
| $K_2O$ | 0.07 | 1.76 | 1.88 | 1.20 |
| $P_2O_5$ | 0.07 | 0.08 | 0.19 | 0.18 |
| LOI | 2.40 | 1.60 | 2.50 | 2.50 |
| $Fe_2O_3t$ | 10.40 | 3.30 | 9.40 | 10.30 |
| Total | 97.40 | 98.50 | 98.60 | 97.90 |
| | | | | |
| Ba | 47 | 635 | 493 | 373 |
| Cr | 19 | | 45 | 196 |
| Cs | 0.03 | 0.41 | 1.20 | 1.70 |
| Cu | 46 | | 35 | 80 |
| Ga | 21.0 | 15.0 | 19.0 | 17.0 |
| Hf | 1.0 | 3.4 | 2.4 | 2.0 |
| Nb | 2.0 | 6.0 | 3.7 | 2.9 |
| Ni | | | 23 | 56 |
| Pb | 4.0 | 13.0 | 2.0 | 4.0 |
| Rb | 0.5 | 55.0 | 43.0 | 26.0 |
| Sc | 27 | 10 | 33 | 37 |
| Sr | 174 | 264 | 276 | 312 |
| Th | 0.81 | 3.90 | 3.50 | 2.50 |
| U | 0.36 | 0.95 | 0.73 | 0.55 |
| V | 214 | 56 | 275 | 277 |
| Y | 15 | 15 | 24 | 21 |
| Zn | 123 | 32 | 51 | 58 |
| Zr | 32 | 132 | 94 | 75 |
| | | | | |
| La | 5.30 | 16.00 | 14.00 | 12.00 |
| Ce | 12.00 | 32.00 | 32.00 | 27.00 |
| Pr | 1.60 | 3.60 | 4.20 | 3.50 |
| Nd | 7.60 | 13.00 | 18.00 | 15.00 |
| Sm | 2.10 | 2.60 | 4.00 | 3.50 |
| Eu | 0.83 | 0.96 | 1.20 | 1.10 |
| Gd | 2.50 | 2.50 | 4.20 | 3.70 |
| Tb | 0.41 | 0.40 | 0.64 | 0.58 |
| Dy | 2.50 | 2.40 | 4.00 | 3.50 |
| Ho | 0.54 | 0.48 | 0.80 | 0.72 |
| Er | 1.50 | 1.30 | 2.20 | 2.00 |
| Tm | 0.23 | 0.23 | 0.35 | 0.31 |
| Yb | 1.50 | 1.40 | 2.20 | 2.00 |
| Lu | 0.24 | 0.25 | 0.36 | 0.33 |